

CHROM. 10,948

## THEORY OF CHROMATOGRAPHY ON HYDROXYAPATITE COLUMNS WITH SMALL LOADS\*

### V. DETERMINATION OF THE ADSORPTION ENERGY OF THE $\epsilon$ -AMINO GROUP OF POLY-L-LYSINE AND THE MANNER OF ADSORPTION OF THE MOLECULE

TSUTOMU KAWASAKI

*Laboratoire de Génétique Moléculaire, Institut de Recherche en Biologie Moléculaire, Faculté des Sciences, Paris 5° (France)*

(First received December 15th, 1977; revised manuscript received February 10th, 1978)

---

#### SUMMARY

In an earlier paper, the energy of adsorption of nucleoside phosphates on to a C site of hydroxyapatite was estimated. In this paper, the theory of chromatography developed for rigid molecules in earlier papers is extended to the case of flexible molecules, and the experimental chromatogram obtained by Bernardi for a low-molecular-weight poly-L-lysine is analysed by using a method similar to that applied to nucleoside phosphates. It is estimated that the energy of adsorption on to a P site for an  $\epsilon$ -amino group of the side-chain of poly-L-lysine is 2–2.2 kcal/mole. It is probable that the feature of interaction among competing or sodium ions near the crystal surface of hydroxyapatite is different from that which occurs in the usual bulk solution. On the basis of a crystallographic study, it can also be deduced that a P site is constructed with six oxygen ions belonging to three crystal phosphates and that P sites are arranged hexagonally on the  $(\vec{a}, \vec{b})$  crystal surface of hydroxyapatite with a minimal distance of 9.42 Å. The manner of the adsorption of poly-L-lysine on an array of P sites is discussed by using space-filling models for both poly-L-lysine and the crystal surface, the latter being constructed on the surface of the plasticine, which is compared with the results obtained from the analysis of the chromatographic data. The chromatographic data for lysozyme and cytochrome *c* discussed in an earlier paper are again discussed on the basis of several parameters obtained in this paper.

---

#### INTRODUCTION

Bernardi<sup>1,2</sup> and Bernardi and Kawasaki<sup>3</sup> concluded that the principal mechanisms of the chromatography of nucleoside phosphates (or nucleic acids) and acidic

---

\* We have omitted the term "rigid molecules" from the title, as the theory has now been extended to the case of molecules with any flexible structures.

polypeptides must be the specific competition of the phosphate and carboxyl groups of these molecules with phosphate ions of the eluent for common adsorbing sites (called C sites<sup>4-7</sup>) of hydroxyapatite (HA)\*. In fact, the elution of these acidic molecules is carried out only by phosphate ions and is hardly influenced by cations or chloride ions in the buffer<sup>1-3</sup>. Bernardi and co-workers<sup>8,9</sup> also concluded, on the basis of the chromatographic data for a number of synthetic polypeptides and proteins with different isoelectric points, that there is a second type of adsorbing site on the surface of HA. These sites (called P sites<sup>4-6</sup>) must adsorb the basic groups of basic polypeptides and basic proteins, and the elution of basic molecules from the HA columns must be due to specific competition of these molecules with cations of the buffer which are also adsorbed on to P sites, because the elution of basic molecules seems to be carried out only by cations (see refs. 8 and 9 and Appendix I in ref. 10)\*\*.

The fact that the elution of acidic and basic molecules is hardly influenced by cations and anions, respectively, of the same buffer (see above) suggests that C and P sites exist in different domains on the crystal surface. The fact that the adsorption capacity of HA for basic proteins is much larger than that for acidic DNA (see Appendix I in ref. 4) also suggests that C and P site domains are separated and that the area of the P site domain is much larger than that of the C site domain. HA crystals prepared for our chromatography have blade-like shapes (see Appendix II in ref. 10)\*\*\*. When a typical basic protein, cytochrome *c*, is adsorbed on HA, the flat surfaces of the crystals, which represent the largest part of the total crystal surfaces, are stained; this indicates that the adsorption of cytochrome *c* and other basic molecules must occur mainly on flat crystal surfaces, and the adsorption of acidic molecules on side faces that occupy only a small proportion of the total crystal surfaces (see Appendix II in ref. 10 and Appendix I in ref. 4). On the other hand, from the measurement of the angles made by two different side faces of the crystals, it is highly probable that  $(\vec{a}, \vec{b})$  planes of unit crystal cells<sup>11-13</sup> appear on flat crystal surfaces and that both  $(\vec{a}, \vec{c})$  and  $(\vec{b}, \vec{c})$  planes<sup>11-13</sup> appear on some of the side faces (see Appendix II in ref. 10).

Taves and Reedy<sup>14</sup> showed, on the basis of a crystallographic study, that both phosphate ions and phosphate groups of the polyphosphate ion (as a part of the

\* To be precise, it should be stated that the mechanism of chromatography is a competition between acid molecules themselves and phosphate ions of the eluent, because the possibility that some crystal sites under an adsorbed molecule are covered by the molecule but are not reacting with phosphate or carboxyl groups of the molecule should be taken into account. The adsorption of phosphate ions of the eluent on to some crystal sites under the adsorbed molecule may be blocked owing to the presence of the molecule, even if they are not occupied by or reacting with acidic groups of the molecule. This is the reason why the value of the parameter  $\xi$  can be less than unity (see later).

\*\* It is difficult to prove directly that anions do not interfere in the elution of basic polypeptide, as it is impossible to perform the experiment by eliminating the anions from the system. However, this is highly probable from the experiment with proteins with different isoelectric points (see Appendix I in ref. 10 and refs. 8 and 9). In contrast to the case with basic molecules, the proof that the elution of acidic molecules is carried out only by phosphate ions of the buffer is much easier and clearer, because chloride ions, although anions, do not interfere in the elution of acidic molecules; it can be shown that elution phosphate molarities of acidic molecules are hardly influenced by the coexistence of KCl and NaCl, except under some extreme experimental conditions<sup>1-3</sup>.

\*\*\* All chromatographic experiments cited in this paper were carried out by using HA crystals prepared by the method of Bernardi<sup>2</sup>, microphotographs of which are shown in Appendix II in ref. 10.

nucleoside phosphate) must be adsorbed on hydroxyl positions devoid of hydroxyl ions existing on the surface of HA. It is assumed that these positions correspond to chromatographic C sites (see above). In Parts I–III of this series<sup>4–6</sup> a theory of chromatography on HA columns with small loads was developed on the basis of the competition model (see above), and in Part IV<sup>7</sup> the experimental chromatogram obtained by Bernardi<sup>15</sup> for a mixture of AMP, ADP, ATP and adenosine tetraphosphate was analysed by using the theory developed earlier<sup>4–6</sup> and on the basis of the model of Taves and Reedy<sup>14</sup> for the adsorption of both phosphate and polyphosphate ions on the crystal surface (see above). By means of this analysis, it was estimated that the adsorption energy on to a C site for a univalent phosphate group on the polyphosphate chain of nucleoside phosphates is 0.9–1 kcal/mole, and that the adenosine group of these molecules covers at most only one crystal site; arguing in the other direction, these reasonable conclusions strongly support the idea of the one-to-one correspondence between a hydroxyl position and a chromatographic C site, and the model of Taves and Reedy<sup>7</sup>. Further, this idea is compatible with the conclusion obtained from the adsorption experiment that acidic molecules must be adsorbed on side faces of the HA crystal that correspond to both  $(\vec{a}, \vec{c})$  and  $(\vec{b}, \vec{c})$  planes (see above), because, according to the Taves and Reedy<sup>14</sup> model, hydroxyl positions devoid of hydroxyl ions must appear on crystal surfaces corresponding to these planes.

In this work, a chromatogram obtained by Bernardi<sup>16</sup> for a low-molecular-weight poly-L-lysine (see Fig. 1) has been analysed with a method similar to that applied in Part IV<sup>7</sup> for the analysis of the chromatogram of the nucleoside phosphates mixture. It is shown that the theory developed in earlier papers<sup>4–7</sup> for molecules with rigid structures is valid for molecules with any flexible structure only if another physical interpretation is given to the parameter  $\sigma$ . It is estimated that the adsorption energy on to a P site for an  $\epsilon$ -amino group on the side-chain of poly-L-lysine is 2–2.2 kcal/mole. The dependence of the activity of competing or sodium ions on the molarity is also discussed; this is different from that observed for the sodium salt in the usual aqueous solution, and it can be suggested that the feature of interactions among sodium ions near the HA surface is different from that which occurs in the usual solution. It can be considered that poly-L-lysine molecules have highly stretched conformations under the experimental conditions (see Appendix I). In Appendix I, the adsorption of poly-L-lysine on the HA surface is discussed. In Appendix II, the HA surface structure, parallel to  $(\vec{a}, \vec{b})$  planes of unit cells (see above), is explored on the basis of crystallographic data. It is probable that a P site is constructed with six oxygen ions (three O<sub>II</sub> and three O<sub>III</sub> ions<sup>11–15</sup>) belonging to three crystal phosphates and that P sites are arranged hexagonally on the crystal surface [corresponding to  $(\vec{a}, \vec{b})$  planes] with a minimum distance of 9.42 Å. In Appendix III, the configuration of poly-L-lysine adsorbed on an array of P sites is again discussed by using space-filling molecular models for both poly-L-lysine and the crystal surface, the latter being constructed on the surface of plasticine. In Appendix IV, the chromatographic data for lysozyme and cytochrome *c* discussed earlier<sup>4</sup> are again discussed on the basis of several results presented in this paper.

## THEORETICAL

*(A) Extension of the theory of chromatography for rigid molecules to the general case of flexible molecules*

The theory of chromatography for rigid molecules developed in earlier papers<sup>4-7</sup> can be extended to the general case of flexible molecules. According to the previous theory<sup>4-7</sup>, the ratio,  $B$ , of the number of molecules in the mobile phase to the total number of molecules in a column section (which is the fundamental factor determining the position of a chromatographic peak) depends upon the factor  $\beta\sigma$  (see eqns. 1 and 2 in ref. 4<sup>\*</sup>) where  $\beta$  is a parameter concerning the properties of the column assuming the activity coefficient for the sample molecule in the column interstices is constant. This is a reasonable assumption, as the concentration of the sample molecule in the column interstices is usually very low, which means that the value of the activity coefficient is virtually unity. Eqn. A1 in Appendix I in ref. 4 shows that  $\beta$  is proportional to the coordination number,  $z$ , of adsorption sites on the crystal surface of HA; the parameter  $B$  therefore depends on the product of  $\sigma$  and  $z$ . Provided that the molecule is rigid and that it is adsorbed in the energetically most stable manner on the surface of HA, the product  $\sigma z$  would represent the number of possible orientations plus configurations of the molecule on the surface of HA. Therefore, if there is only one energetically most stable configuration,  $\sigma$  is the symmetry factor of the molecule, the value of which can lie between  $1/z$  and 1, and is unity for the usual asymmetric molecule. If there are  $n$  energetically most stable configurations of the molecule, the value of  $\sigma$  should be  $n$  times as large. It can also be considered that the factor  $-x\varepsilon - kT \ln(z\sigma)$ , the value of which is different from that of the factor  $-\ln q$  in eqn. 1 in ref. 4 by a constant value, and where  $x\varepsilon$ <sup>\*\*</sup> represents the adsorption energy per molecule, represents a type of free energy of adsorption per molecule. In general, the configuration of the molecule on the crystal surface would follow a Boltzmann distribution and the molecule would be adsorbed virtually in the energetically most stable configuration only if the value of the adsorption energy,  $\varepsilon$ , per adsorption group of the molecule is large enough. Therefore, the general physical meaning of the factor  $z\sigma$  for the rigid molecule would be the approximate number of possible orientations plus configurations of the molecule on the crystal surface, provided that the value of the factor  $-x\varepsilon - kT \ln(z\sigma)$  is close to the minimum. More precisely, values of both  $\sigma$  and  $-x\varepsilon - kT \ln(z\sigma)$  must be relevant to the water structure near the crystal surface. It is easy to understand that the theory developed in earlier papers<sup>4-7</sup> can be extended to the general case of flexible molecules if, in this instance, a physical meaning of the approximate number of the possible orientations and configurations plus possible stereochemical conformations of the molecule is assigned to the parameter  $z\sigma$ ; as above, the factor  $-x\varepsilon - kT \ln(z\sigma)$  should be close to the minimum.

*(B) Interpretation of the experimental chromatogram of poly-L-lysine*

It can be seen in Fig. 1 that the chromatogram of a low-molecular-weight poly-L-lysine hydrobromide (for details of the molecule, see the legend of Fig. 1)

\* In some instances in ref. 4, the symbol  $\beta_3$  was used instead of  $\beta$ .

\*\* In ref. 4, the symbol  $\varepsilon_3$  was used instead of  $\varepsilon$ .

contains a sharp peak (peak 1) that appears before the molarity gradient of sodium ions begins and a series of peaks (peaks 2-9) that are eluted at different sodium molarities. The intervals between the latter peaks are roughly constant, and the heights of peaks decrease gradually on the right-hand side of the chromatogram. On the left-hand side, they begin to decrease but stop abruptly.

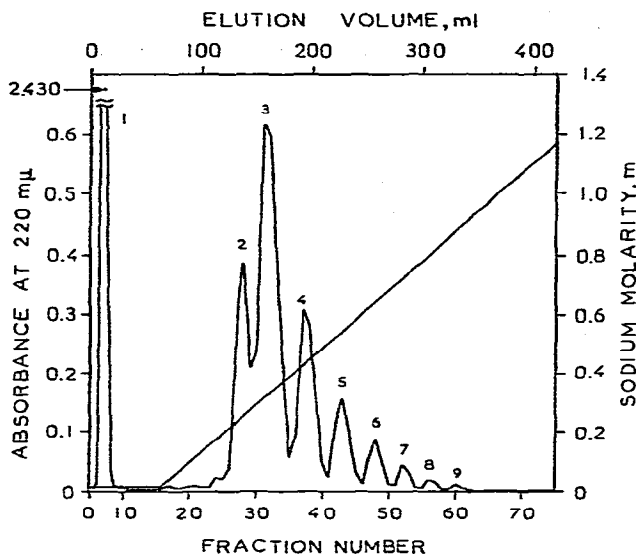


Fig. 1. Chromatography, at room temperature, of a poly-L-lysine·HBr sample [Miles-Yeda, code No. 8120A (new code No. 71-120A) lot No. LY125] with molecular weights between 1500 and 8000, *i.e.*, with degrees of polymerization of 7-38. Fifty-nine  $A_{220}$  units, or 20 mg as estimated by using Fig. 10.1 in ref. 17, of the sample in 4 ml of 0.01 *M* sodium phosphate buffer of pH 6.8 (NaP) were loaded at zero volume on a  $22 \times 1$  cm HA column. After rinsing the column with 30 ml of 0.01 *M* NaP, elution was carried out with a linear molarity gradient of NaP constituted by three 150-ml solutions of 0.01, 0.5 and 1 *M* NaP. The yields were 23% and 50%, respectively, for peak 1, which is not retained on the column, and for the other part of the chromatogram including peaks 2-9 that elutes after the molarity gradient begins, with an overall recovery of 73%. The number of molecules involved in the latter part of the chromatogram, which can be estimated to be equivalent to 10 mg (see above), would be small enough (for a  $22 \times 1$  cm column) for the effect of mutual interactions among molecules adsorbed on HA or the mutual displacement of molecules<sup>18</sup> to be virtually negligible (*cf.*, Fig. 3 in ref. 19, from which it can be estimated that the maximum possible displacement of the elution molarity is of the order of 0.02 *M*). Some other information involved in the figure is given in Table I. [This figure was reproduced with slight modifications from Fig. 5a in ref. 16, where it is mentioned that potassium buffer was used (instead of sodium buffer) and that the maximum height of peak 1 is 2.067 (instead of 2.430), which are misprints. Some information not given in ref. 16 but only in this paper was obtained directly from the original data with the permission of Prof. G. Bernardi].

It can be shown theoretically that, with sufficiently small molecules, the elution molarity is governed mainly by the parameter  $x$  rather than by the parameter  $\xi (= x/x')^*$ , where  $x$  is the number of adsorption groups per molecule that react with sites of HA and  $x'$  is the number of sites of HA where competing ions cannot be adsorbed owing to the presence of an adsorbed molecule; this means that peaks

\* With large molecules, the elution molarity is governed by the parameter  $\xi$ .

that appear at high sodium molarities involve molecules with high  $x$  values or high molecular weights. As it can be considered that poly-L-lysine is adsorbed on P crystal sites by using  $\epsilon$ -amino residues of side-chains (for details, see Appendix I and Discussion), the discrete distribution of peaks (Fig. 1) must be a reflection of a stepwise variation in numbers of  $\epsilon$ -amino groups per molecule that react with P sites. It can also be assumed that the gradual decrease in the heights of the peaks on the right-hand side of the chromatogram (as in a binominal distribution) reflects a statistical property concerning the distribution of the polypeptide chain lengths of the poly-L-lysine sample. A similar consideration was made in earlier papers<sup>10,20</sup> for the interpretation of the chromatogram of tropocollagen. The reason why the distribution of the peaks that appear in the sodium gradient stops abruptly on the left-hand side (see Fig. 1) can be understood, for poly-L-lysine, by assuming that for small components the total energy per molecule of the interaction with P sites is too small to be retained on the column, and that these molecules are involved in peak 1, which appears before the sodium gradient begins (see Fig. 1). The possibility that the asymmetry of the distribution of peaks 2-9 is due to mutual interactions among macromolecules on the crystal surface, as considered in earlier papers (e.g., refs. 10, 18, 20 and 21) can almost be excluded, as the load of the sample is small (see the legend of Fig. 1).

Now, the fact that the width of peak 1 is very narrow (see Fig. 1) indicates that the value of  $x$  for molecules involved in this peak is almost constant. The situation is the same as for peaks 2-9 (see above). The fact that the height or the area of peak 1 is (much) larger than that of peak 2, and that the total chromatogram including peak 1 has two maxima (see Fig. 1), suggests that the value of  $x$  for molecules involved in peak 1 is the minimum possible value that can be realized, because the statistical distribution must have only one maximum unless there is a reason for the distribution to be limited\*. It follows from this that the number,  $x$ , of  $\epsilon$ -amino groups per molecule that react with P sites must be (approximately; see Discussion) 1, 2, ..., 9 for molecules involved in peaks 1, 2, ..., 9, respectively, because the minimum possible value of  $x$  is (approximately; see Discussion) unity. Further, if the value of  $x$  for molecules involved in peak 1 is equal to or greater than about 2, it is difficult to explain why only peak 1 elutes before the sodium gradient begins; in order for this to occur, the ratio of the adsorption energy (or the value of  $x$ ) for a molecule involved in peak 2 to the energy (or the value of  $x$ ) for a molecule in peak 1 must be much greater than the ratios of the energies (or values of  $x$ ) between molecules involved in the other pairs of successive peaks (for details of the argument for values of  $x$ , see Discussion).

Finally, it is reasonable to assume that all molecules of poly-L-lysine have almost identical values of the parameter  $\xi$ ; this means that the value of  $x$  or the adsorption energy per molecule increases linearly with the increase in the value of  $x'$  or the dimensions of the molecule.

---

\* It can be shown that the fraction number that corresponds to the centre of gravity of the total chromatogram including peak 1, i.e., the average fraction number between 30 and 31, is almost identical with the fraction number that corresponds to the maximum height of the chromatogram eluting in the sodium gradient, i.e., 30; this also suggests that the poly-L-lysine sample is a statistical assembly of components with different chain lengths and that components with minimum possible values of  $x$  are involved in peak 1.

*(C) Methods for the estimation of the value of the adsorption energy for an  $\epsilon$ -amino group of poly-L-lysine and other experimental parameters*

In Part IV<sup>7</sup>, the value of the adsorption energy on to a C crystal site for a univalent phosphate group on the polyphosphate chain of nucleoside phosphates, the value of the proportionality constant,  $\varphi'$ , between the parameter  $A$  (see ref. 7) and the molarity,  $m$ , relating to phosphate ions of the eluent etc. were estimated from the chromatogram for a mixture of AMP, ADP, ATP and adenosine tetraphosphate (Fig. 3 in ref. 7). We can find the following parallels between the chromatography of nucleoside phosphates (Fig. 3 in ref. 7) and that of poly-L-lysine (Fig. 1): firstly, whereas with nucleoside phosphates there was a difference of unity in numbers of univalent phosphate groups adsorbed on C sites between molecules involved in successive chromatographic peaks (*i.e.*, between AMP and ADP, between ADP and ATP, and between ATP and adenosine tetraphosphate; see Table I in ref. 7), with poly-L-lysine there is also a difference of unity (not always precisely unity; see Discussion) in the numbers of  $\epsilon$ -amino groups adsorbed on P sites between molecules involved in successive peaks in Fig. 1 (see Section B). Secondly, whereas with nucleoside phosphates there was a difference of unity in numbers of C sites on which phosphate ions cannot be adsorbed owing to the presence of an adsorbed molecule between nucleoside phosphates involved in successive peaks (see Table I in ref. 7), with poly-L-lysine there is a difference of almost  $1/\xi$  in the numbers of P sites on which sodium ions cannot be adsorbed owing to the presence of a molecule between components involved in successive peaks, because any molecules of poly-L-lysine must have almost identical values of the parameter  $\xi$  (see Section B). From these parallels it can be understood that the value of the adsorption energy,  $\epsilon$ , for an  $\epsilon$ -amino group of poly-L-lysine on to a P crystal site, the value of the parameter  $\varphi'$  for sodium ions, etc., can be estimated from Fig. 1 if the value of the parameter  $\xi$  is given, and if the parameter  $A$  and the molarity  $m$  relating to sodium ions in the eluent are proportional to each other.

The assumption of the proportionality between  $A$  and  $m$  (see above) is unreasonable, however, with poly-L-lysine, because molecules elute over a range of high sodium molarities (0.25–0.9  $M$ ) (see Fig. 1), in contrast to the case with nucleoside phosphates, which elute at phosphate molarities lower than 0.3  $M$  (see Fig. 3 in ref. 7). Nevertheless, it is possible to calculate apparent values of the parameters  $\epsilon$ ,  $\varphi'$ , etc., from any pair of successive peaks in Fig. 1\* if the parameter  $\varphi'$  in the term  $\varphi' m_{in}$  in eqn. 1 in ref. 7 is replaced with the ratio,  $\varphi'_{in}$ , of  $A$  to  $m$  when  $m$  is equal to its initial value of  $m_{in}$  ( $= 0.015 M$ ) (see Table I; for the method of evaluation of the parameter  $\varphi'_{in}$ , see below). As  $A$  and  $m$  must be proportional to each other when  $m$  is close to zero, if both parameters  $\varphi'_{in}$  and  $\xi$  are given, and if apparent values of  $\epsilon$ ,  $\varphi'$ , etc., obtained from different pairs of peaks that appear at different (average) sodium molarities are extrapolated to zero molarity, then the true value of the parameter  $\epsilon$ , the value of the parameter  $\varphi'$  at  $m = 0$  (called  $\varphi$ ), etc., can be obtained.

Now, provided that only the value of  $\xi$  is given, the value of  $\varphi'_{in}$  can be estimated as follows. For a hypothetical value of  $\varphi'_{in}$ , apparent values of  $\varphi'$  are cal-

\* With nucleoside phosphates, values of the corresponding parameters were calculated from the pair of chromatographic peaks of ATP and adenosine tetraphosphate<sup>7</sup>.

TABLE I  
DATA INVOLVED IN FIG. 1.

Parameter	Symbol*	Value	Notes**
Column length	$L$	22 cm	
Column diameter	$\emptyset$	1 cm	
Slope of sodium molarity gradient (molarity per elution volume)	grad	0.0033 M/ml	1
Interstitial volume per unit length of column	$v$	0.628 ml/cm	2
Total interstitial volume of column	$V_T$	13.816 ml	
Slope of sodium molarity gradient (molarity per column length)	$g$	0.00207 M/cm	2
Product of $g$ and $L$	$s$	0.0456 M	
Molarity of sodium ions before the gradient begins	$m_{in}$	0.015 M	3
Volume of solvent eluted from the sample load until the gradient begins	$V'$	66 ml	
Temperature	$T$	Room temperature	4
Elution volume at the maximum height of the peak 1		12 ml	
Elution sodium molarity at the maximum height			
of peak 2		0.24 <sub>8</sub> M	
of peak 3		0.30 <sub>8</sub> M	
of peak 4		0.42 <sub>5</sub> M	
of peak 5		0.54 <sub>5</sub> M	
of peak 6		0.64 <sub>2</sub> M	
of peak 7		0.72 <sub>0</sub> M	
of peak 8		0.80 <sub>0</sub> M	
of peak 9		0.87 <sub>7</sub> M	

\* Some of the symbols do not appear in the text, but they are shown here in order to facilitate comparison of this paper with Part IV<sup>7</sup>.

\*\* Notes: (1) Note that the gradient is not expressed in terms of the phosphate molarity but of the sodium molarity, because poly-L-lysine competes with sodium ions of the buffer (see text). (2) See Table II in ref. 7. (3) This is the approximate value in elution volumes immediately before the sodium gradient begins; cf., ref. 7. (4) If necessary for the calculation, this is assumed to be 25 °C.

culated from different pairs of peaks appearing at different sodium molarities. These values of  $\varphi'$  are extrapolated to  $m = m_{in}$ . The extrapolated value of  $\varphi'$ ,  $\varphi'_{(m=m_{in})}$ , must, in general, be different from the initially assumed value of  $\varphi'_{in}$ . Calculations are repeated until the value of  $\varphi'_{in}$  that produces a value of  $\varphi'_{(m=m_{in})}$  identical with itself is found, which must be the true value of  $\varphi'_{in}$ . Actually, the value of  $\varphi'_{in}$  is virtually equal to the value of  $\varphi$  (see above), because the value of  $m_{in}$  (0.015 M) is close to zero (see Results of Calculations).

As values of  $\varepsilon$ ,  $\varphi'_{in}$  ( $\approx \varphi$ ), etc., were calculated when the value of  $\xi$  was given, it is possible to determine the empirical formula of the function  $\varphi'(m)$  (which fulfils the relationship  $\varphi' = \varphi'_{in}$  when  $m = m_{in}$  for any given value of  $\xi$ ) in such a way that the positions of peaks 2-9 of poly-L-lysine calculated by using this function would be equal to those obtained experimentally. It will be shown that, for any reasonable value of  $\xi$ ,  $A$  is proportional to  $m$  (i.e.,  $\varphi'$  is constant) when  $m$  is small enough.

Now, we must estimate the value of  $\xi$ . It can be considered that the value of  $\varphi'e^{-\varepsilon'/kT}$ , where  $\varepsilon'$  is the adsorption energy of a competing ion on to a crystal



site, is independent of the type of competing ions when the molarity,  $m$ , of the ions is low enough, because  $\varphi'e^{-\varepsilon'/kT}$  is proportional to the activity coefficient of the ions\*. Both the (average) value of  $\varphi'$ , when  $m$  is small, for phosphate ions of the buffer and the value of the adsorption energy for a univalent phosphate group on the polyphosphate chain of nucleoside phosphates are known (see above). In order to estimate the value of  $\xi$ , the following assumptions must be made: (1) the adsorption energy for a univalent phosphate ion of the buffer (the phosphate buffer at pH 6.8 used in the experiment is an equimolar mixture of univalent and divalent phosphate ions) is equal to the energy for a univalent phosphate group on the polyphosphate chain of the nucleoside phosphate; (2) the adsorption energy for a divalent phosphate ion of the buffer is twice as large as the energy for a univalent ion; (3) the proportion of univalent and divalent ions adsorbed on the crystal surface follows the Boltzmann distribution; (4) the (average) value of  $\varphi'e^{-\varepsilon'/kT}$  calculated for phosphate ions on the basis of assumptions (1)–(3) is virtually equal to the limiting value when  $m$  tends to zero; and (5) the adsorption energy for a sodium ion is virtually equal to the energy for an  $\varepsilon$ -amino group of poly-L-lysine (because both the sodium ion and the  $\varepsilon$ -amino group have a univalent charge). The value of the parameter  $\xi$  can now be estimated in such a way that the value of  $\varphi e^{-\varepsilon/kT}$  [i.e.,  $e^{-\varepsilon/kT} \lim_{m \rightarrow 0} \varphi'(m)$ ] for sodium ions obtained by using assumption (5) and the hypothetical value of  $\xi$  be equal to the (average) value of  $\varphi'e^{-\varepsilon'/kT}$  obtained for phosphate ions. Hence, values of parameters  $\varepsilon$ ,  $\varphi$  ( $\approx \varphi'_{in}$ ), etc., and the empirical formula of the function  $\varphi'(m)$  can finally be determined. (For details of the method, see Results of Calculations).

## RESULTS OF CALCULATIONS

Fig. 2 illustrates an example of calculations of apparent values of  $\varphi'$ ,  $\varepsilon$ ,  $\beta\sigma e^{\varepsilon_0/kT}$ ,  $\varepsilon_0$  and  $\beta\sigma$  (for the definition of  $\varepsilon_0$  and methods of calculations of  $\varepsilon_0$  and  $\beta\sigma$ , see below) obtained on the basis of elution molarities of seven different pairs of successive peaks in Fig. 1 (i.e., peaks 2 and 3, peaks 3 and 4, ..., peaks 8 and 9), and by assuming  $\xi = 1/2$  and  $\varphi'_{in} = 10$ . In Fig. 2, the abscissa is the molarity of sodium ions and dotted vertical lines indicate the positions of the maximum heights of peaks 2–9 in Fig. 1. As  $\xi = 1/2$  and  $\xi = x/x'$ , the values of  $x'$  for molecules involved in peaks 2–9 must be equal to 4, 6, ..., 18, respectively; pairs of closed circles on different levels indicate pairs of peaks chosen as the basis of calculations of apparent values of the parameters. From a pair of peaks, two apparent values of  $\varphi'$  and two apparent values of  $\varepsilon$  (or the adsorption energy for an  $\varepsilon$ -amino group as the difference in the apparent adsorption energies between molecules involved in successive peaks) can be calculated, at the same time with apparent elution molarities for the right- and the left-hand neighbour peaks of the pair chosen as the basis of the calculation, which are shown by open circles in Fig. 2\*\*. In fact, if the value of

\*  $\varphi' = \Lambda/m$  and  $\Lambda = \lambda e^{\varepsilon'/kT}$ , where  $\lambda$  is the absolute activity of competing ions. Therefore, we have  $\varphi' e^{-\varepsilon'/kT} = \lambda/m$ ,  $\lambda/m$  being proportional to the activity coefficient<sup>4</sup>.

\*\* In ref. 7,  $\varphi'$ ,  $\varepsilon$  and  $\beta\sigma e^{\varepsilon_0/kT}$  were calculated at the same time only with the elution molarity for the left-hand neighbour peak of the basic pair, i.e., they were calculated at the same time with the theoretical elution molarity for the peak of ADP by choosing peaks of ATP and adenosine tetraphosphate as the basic pair. The fact that these parameters can also be calculated at the same time with the elution molarity for the right-hand neighbour peak is proved in the Appendix in ref. 7.

$\varphi'$  is independent of the sodium molarity and if values of both  $\xi$  and  $\varphi'_{in}$  are correctly assumed, then open circles (see above) must be superposed on the dotted vertical lines, and values of both  $\varphi'$  and  $\epsilon$  calculated at the same time with theoretical elution molarities of the right- and the left-hand peaks of the basic pair must be equal to each other; this means that values of both  $\varphi'$  and  $\epsilon$  calculated from any basic pairs of peaks must also be equal to one another. In parentheses above and below the other values in the tabular matter to the right side of Fig. 2 are given values of  $\varphi'$  and  $\epsilon$  obtained concomitantly with positions of open circles on the right- and the left-hand sides of the pair of closed circles, respectively; the values between those in parentheses are the means of the values of  $\varphi'$  and  $\epsilon$  given in parentheses. The fact that the values of both  $\varphi'$  and  $\epsilon$  depend not only on whether the molarity for the right- or the left-hand peak is calculated at the same time but also on which pair of the peaks is chosen as the basis of the calculation would indicate that the value of  $\varphi'$  depends on the sodium molarity or/and that the hypothetical value of  $\xi$  is incorrect (see above)\*. It can be considered, however, that the dependences of apparent values of  $\varphi'$  and  $\epsilon$  on the method of the calculation are mainly due to the dependence of the value of  $\varphi'$  on the sodium molarity because, for any reasonable hypothetical values of  $\xi$ , values of both  $\varphi'$  and  $\epsilon$  depend in similar ways on the method of calculation.

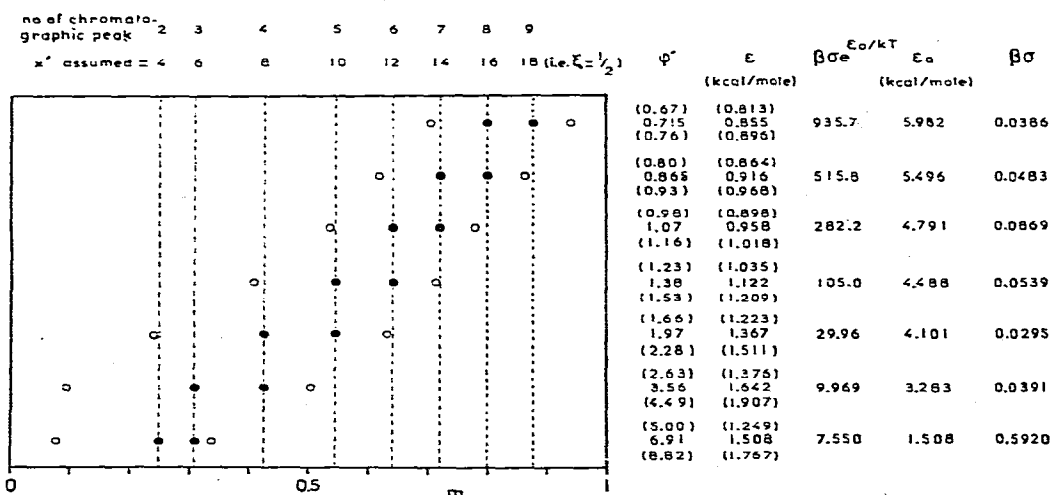


Fig. 2. Example of calculations of apparent values of  $\varphi'$ ,  $\epsilon$ ,  $\beta\sigma e^{\epsilon_0/kT}$ ,  $\epsilon_0$  and  $\beta\sigma$  obtained on the basis of the elution molarities of seven different pairs of successive peaks in Fig. 1 (i.e., pairs of peaks 2 and 3, peaks 3 and 4, ..., peaks 8 and 9), and by assuming  $\xi = 1/2$  and  $\varphi'_{in} = 10$ .

On the right of Fig. 2 are tabulated values of  $\beta\sigma e^{\epsilon_0/kT}$  calculated from the seven pairs of chromatographic peaks in Fig. 1 by using a method similar to that in ref. 7, where  $\epsilon_0$  is the apparent adsorption energy for molecules involved in the left-hand neighbour peak of the pair chosen as the basis of the calculation; apparent

\* The value of  $\varphi'_{in}$  chosen here is that which should be true provided the hypothetical value of  $\xi$  is true (see Theoretical, Section C, and below).

values of both  $\varepsilon_0$  and  $\beta\sigma$  calculated by assuming  $\varepsilon_0 = x\varepsilon^*$  are also tabulated, where  $\varepsilon$  is the mean value shown between the values in parentheses in the second column. It can be seen from the table in Fig. 2 that the values of all of the parameters  $\varphi'$ ,  $\varepsilon$ ,  $\beta\sigma e^{\varepsilon_0/kT}$  and  $\varepsilon_0$  change monotonously from top to bottom in the respective columns except for the value of  $\varepsilon$  calculated from the pair of peaks 2 and 3. It can also be seen that the value of  $\beta\sigma$  is always of the order of  $10^{-2}$  when the basic pairs of peaks for the calculation are chosen from peaks 3-9; it is exceptionally high when the pair of peaks 2 and 3 is chosen as the basis of the calculation, however. It can be considered that this exceptionally high value of  $\beta\sigma$  is related to the fact that the interval between peaks 2 and 3 is very narrow or that the elution molarity of peak 2 is too high (for an explanation of the elution molarity of peak 2, see Discussion).

The points in Fig. 3 are logarithms of mean values of  $\varphi'$  shown between the values given in parentheses in the first column of the table in Fig. 2 versus mean elution molarities for pairs of peaks used as the basis of the calculations of corresponding  $\varphi'$  values; the value of  $\varphi'$  calculated from peaks 2 and 3 is not plotted, as the position of peak 2 is exceptional (see above). The intermediate straight line in Fig. 3 is the regression line for  $\ln\varphi'$  on  $m$  obtained by the least-squares method for the points in the same figure; the upper and the lower broken lines are regression lines for corresponding points (not shown) obtained by assuming that  $\varphi'_{in} = 14$  and  $\varphi'_{in} = 6$ .

The three points in Fig. 4 are the exponents of the ordinate values of the three regression lines at  $m = m_{in}$  ( $= 0.015 M$ ) in Fig. 3 [denoted by  $\varphi'_{(m=m_{in})}$ ] versus

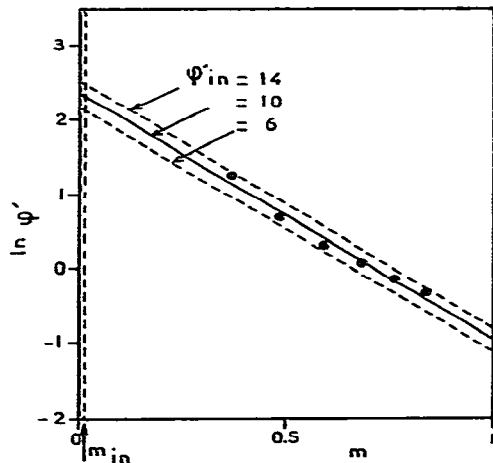


Fig. 3. Points: plots of logarithms of mean values of  $\varphi'$  shown between the upper and lower values in parentheses in the first column of the table in Fig. 2 versus mean elution molarities of pairs of peaks used as the basis of calculations of corresponding  $\varphi'$  values. The values of  $\varphi'$  calculated from peaks 2 and 3 are not plotted, as the position of peak 2 is exceptional. The intermediate line is the regression line for these points; the upper and the lower broken lines are regression lines for corresponding points (not shown) obtained by assuming  $\varphi'_{in} = 14$  and  $\varphi'_{in} = 6$  instead of  $\varphi'_{in} = 10$ .

\* It is also assumed that values of  $x$  involved in peaks 2, 3, ..., 9 are exactly equal to 2, 3, ..., 9, respectively. For the validity of this assumption, see Discussion.

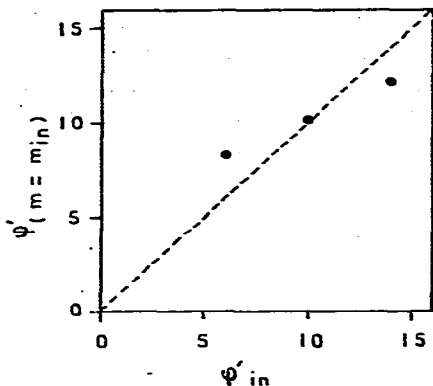


Fig. 4. Points: plots of the exponents of ordinate values of the three regression lines at  $m = m_{in}$  ( $= 0.015 M$ ) in Fig. 3 [denoted by  $\varphi'_{(m=m_{in})}$ ] versus the corresponding  $\varphi'_{in}$  values. It can be seen that the value of  $\varphi'_{(m=m_{in})}$  coincides with the value of  $\varphi'_{in}$  when  $\varphi'_{in} \approx 10$ .

the corresponding  $\varphi'_{in}$  values. It can be seen from Fig. 4 that the value of  $\varphi'_{(m=m_{in})}$  coincides with that of  $\varphi'_{in}$  when  $\varphi'_{in} \approx 10$ , which means that the value of  $\varphi'_{in}$  should be 10 if  $\xi = 1/2$  (see Theoretical, Section C).

The points and the crosses in Fig. 5 are apparent values of  $\epsilon$  (mean values shown between the values given in parentheses in Fig. 2) and  $\beta\sigma$  in the table in Fig. 2 versus the mean elution molarities of pairs of peaks used as the basis of the calculations of  $\epsilon$  and  $\beta\sigma$ , where  $\xi = 1/2$  and  $\varphi'_{in} = 10$ ; values of  $\epsilon$  and  $\beta\sigma$  calculated from the pair of peaks 2 and 3 are not plotted, as in Fig. 3. The oblique straight line in

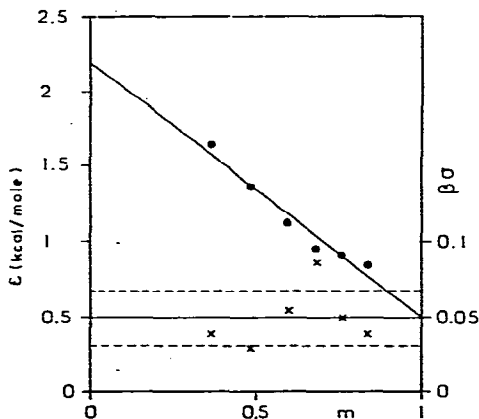


Fig. 5. Symbols: plots of apparent values of (●)  $\epsilon$  (mean values shown between the upper and lower values in parentheses) and (×)  $\beta\sigma$  in the table in Fig. 2 versus mean elution molarities of pairs of chromatographic peaks used as the basis of calculations of corresponding  $\epsilon$  and  $\beta\sigma$ , respectively. Values of  $\epsilon$  and  $\beta\sigma$  calculated from the pair of chromatographic peaks 2 and 3 are not plotted, as the position of peak 2 is exceptional. The oblique straight line is the regression line for the points, from which it can be estimated that the value of  $\epsilon$  extrapolated to  $m = 0$  is 2.2 kcal/mole, which must be the true value (provided  $\xi = 1/2$ ); the horizontal continuous and two broken lines indicate the mean value and the range of the standard deviation of the apparent values of  $\beta\sigma$ , respectively. It is assumed that the mean value is roughly equal to the true value of  $\beta\sigma$ .

Fig. 5 is the regression line for apparent values of  $\varepsilon$  on  $m$  obtained by the least-squares method for the points in the same figure, from which it can be estimated that the value of  $\varepsilon$  extrapolated to  $m = 0$  is 2.2 kcal/mole, which must be the true value (provided  $\xi = 1/2$ ); the horizontal continuous line and the two broken lines indicate the mean value and the range of the standard deviation of the apparent values of  $\beta\sigma$ , respectively, and we assume simply that the mean value is about equal to the true value of  $\beta\sigma$ , which is a rough approximation. However, the considerable random variation of the apparent values of  $\beta\sigma$  around the mean value in Fig. 5 suggests that the chromatography does not depend substantially on the value of  $\beta\sigma$ , which can be verified (see below).

Now, it is possible to calculate theoretical positions of the peaks in Fig. 1 by using values of parameters  $\varphi'_{in}$ ,  $\varepsilon$  and  $\beta\sigma$  estimated above with the assumption that  $\xi = 1/2$ , and also by assuming several empirical equations for the function  $\varphi'(m)$ , which should fulfil a condition such that  $\varphi' = \varphi'_{in}$  when  $m = m_{in}$ . As the function  $\varphi'(m)$  should be related to the activity coefficient of competing ions (see below), a simple assumption for this function may be that

$$\varphi'(m) = \varphi\gamma' \quad (1)$$

where

$$\gamma' = e^{-\alpha R(m)} \quad (2)$$

and  $\alpha$  is a constant. If the dependence of  $\varphi'$  on  $m$  is essentially due to the dependence of the activity of competing ions on the molarity in the column interstices far enough from HA surfaces for it not to be influenced by HA surfaces, then the parameter  $\gamma'$  in eqn. 1 should be equal to the activity coefficient,  $\gamma$ , for the ions in the usual aqueous solution (see Discussion). The curves in Fig. 6 represent theoretical elution molarities for peaks 2-9 in Fig. 1 as functions of the parameter  $\alpha$  in eqn. 2 calculated by assuming 1/2 for the value of  $\xi$  and three different equations for the function  $R(m)$ :

$$R(m) = \sqrt{m} \quad (3a)$$

$$R(m) = m \quad (3b)$$

or

$$R(m) = m^2 \quad (3c)$$

The broken vertical lines in Fig. 6 represent the positions of the maximum heights of peaks 2-9 in Fig. 1. It can be shown by using the same model that the adsorption energy for molecules involved in peak 1 is too small for them to be retained on the column and that these molecules elute at a volume of 34.9 ml, which explains qualitatively the fact that it is only peak 1 that elutes before the gradient of sodium ions begins (see Fig. 1). The theoretical elution volume of peak 1 is larger than the experimental value of 12 ml (see Table I), however, and this will be reconsidered in the Discussion. It can be seen from Fig. 6 that a best fit between the theoretical and experimental elution molarities for molecules retained on the column is obtained only when  $R(m) = m$  and when  $\alpha = 0.9$ , except for the position of peak 2. In the above, we assumed, for the value of  $\beta\sigma$ , the mean value 0.049 of the apparent values

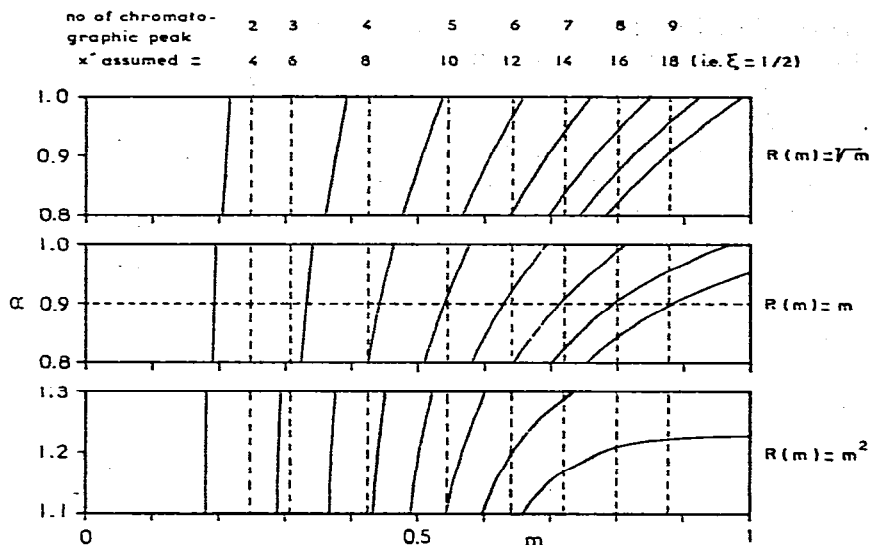


Fig. 6. Theoretical elution sodium molarities for peaks 2-9 in Fig. 1 (abscissa) as functions of the parameter  $\alpha$  in eqn. 2 (ordinate) calculated by assuming  $\xi = 1/2$  and three different equations for the function  $R(m)$ . The vertical broken lines are positions of the maximum heights of peaks 2-9 in Fig. 1. It can be seen that the best fit between the theoretical and experimental values is obtained only when  $R(m) = m$  and  $\alpha = 0.9$ , except for the position of peak 2.

of this parameter in Fig. 5. Similar results are obtained if both extreme values (0.031 and 0.068) of the range of the standard deviation of the apparent values (Fig. 5) are assumed for  $\beta\sigma$ : it is only peak 1 that elutes before the sodium gradient begins and it appears at elution volumes of 27.0 and 42.3 ml if  $\beta\sigma = 0.031$  and 0.068, respectively; it is only when  $R(m) = m$  and  $\alpha = 0.96$  and 0.86 that best fits between the theoretical and experimental results are obtained with respect to the elution molarities of peaks 3-9 if  $\beta\sigma = 0.031$  and 0.068, respectively, the interval between peaks 2 and 3 calculated theoretically always being larger than the empirical value.

If different values of  $2/3$  and  $1/3$  are assumed for  $\xi$ , different values are obtained for  $\varphi'_{in}$ ,  $\varepsilon$  and  $\beta\sigma$  (see Table II), but it is also when  $R(m) = m$  that the best fits between theoretical and experimental results are obtained with respect to the elution molarities of peaks 3-9; in these instances, also, the interval between peaks 2

TABLE II

VALUES OF  $\varepsilon$ ,  $\beta\sigma$ ,  $\varphi'_{in}$  ( $\approx \varphi$ ) AND  $\alpha$  ESTIMATED FOR SEVERAL HYPOTHETICAL VALUES OF  $\xi$

$\xi$	$\varepsilon$ (kcal/mole)	$\beta\sigma$	$\varphi'_{in}$ ( $\approx \varphi$ )	$\alpha^*$
1	$\geq 2.2$		$\geq 50$	
2/3	2.03	$0.070 \pm 0.022$	15	0.87 (0.82, 0.91)
1/2	2.20	$0.049 \pm 0.018$	10	0.90 (0.86, 0.96)
1/3	2.63	$0.024 \pm 0.012$	7	0.97 (0.94, 1.03)

\* The left- and the right-hand values in parentheses are those derived by assuming the upper and the lower limits, respectively, of  $\beta\sigma$  in the third column.

and 3 calculated theoretically is larger than the experimental value; it is only peak 1 that elutes before the sodium gradient begins and the theoretical elution volumes for peak 1 are larger than the experimental value, being 28.7–42.7 ml if  $\xi = 2/3$  and 24.3–45.1 ml if  $\xi = 1/3$ . Fig. 7 is the corresponding figure to Fig. 6 for the case when  $\xi = 2/3$ . If it is assumed that  $\xi = 1$ , it is difficult to estimate the exact value of  $\varphi'_{in}$ . In this instance, in plots corresponding to those in Fig. 4, the points approach so closely to the straight line  $\varphi'_{(m=m_{in})} = \varphi'_{in}$  that the points and the straight line are almost superposed when  $\varphi'_{in} \gtrsim 50$ , from which it can be estimated (*cf.*, Fig. 5) that  $\varepsilon \gtrsim 2.2$  kcal/mole, because the value of  $\varepsilon$  increases monotonously with increase in  $\varphi'_{in}$ . Table II summarizes the results of the calculations obtained so far.

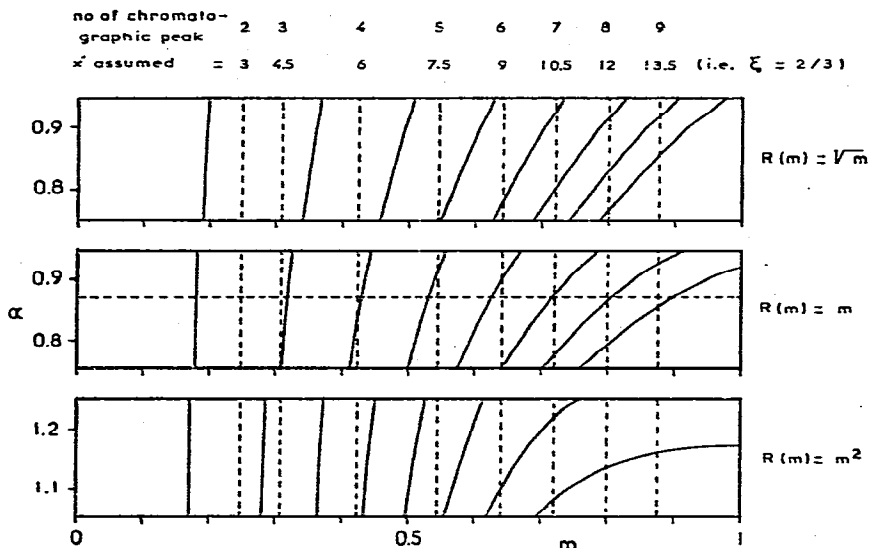


Fig. 7. As Fig. 6, but assuming  $\xi = 2/3$ . In this instance also it is only when  $R(m) = m$  but  $\alpha = 0.87$  that the best fit between the theoretical and experimental values is obtained, except for the position of the peak 2.

In Fig. 8, the parameter  $\gamma'$  (see eqns. 2 and 3b) for three different hypothetical values of  $\xi$  ( $2/3$ ,  $1/2$  and  $1/3$ ) and optimal  $\alpha$  values (see Table II) are plotted as functions of the molarity of sodium ions in the eluent. In Fig. 8, mean activity coefficients ( $\gamma$ ) for both sodium chloride and potassium chloride measured in the usual aqueous solutions (cited from ref. 22) are plotted as functions of the molarities of these salts. It can be suggested that the different behaviours of  $\gamma'$  and  $\gamma$  are mainly due to different (average) features of the interactions of the ions between the interstices of the HA column and the usual bulk solution (see Discussion).

Fig. 9 illustrates the relationships between  $\Delta (= \varphi'm$ ; see ref. 4) and  $m$  calculated by using the functions  $\gamma'(m)$  shown in Fig. 8 for three different values of  $\xi$ . It can be seen from Fig. 9 that there are almost linear relationships between  $\Delta$  and  $m$ , for any values of  $\xi$ , if the sodium concentration is lower than *ca.*  $10^{-1} M$ .

We discussed above possible values of  $\varphi'_{in}$ ,  $\varepsilon$  and  $\beta\sigma$  and possible equations for  $\varphi'(m)$  for some hypothetical values of  $\xi$ . We must now estimate the value of

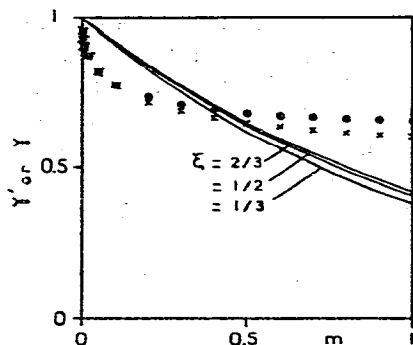


Fig. 8. Curves: plots of  $\gamma'$  (eqn. 2) as functions of the sodium molarity for three different hypothetical values of  $\xi$  and best  $\alpha$  values (see Table II). Symbols: plots of activity coefficients ( $\gamma$ ) of (●) NaCl and (×) KCl at 25 °C as functions of salt molarities. It can be suggested that the different behaviours of  $\gamma'$  and  $\gamma$  are mainly due to different (average) features of interactions of ions between the interstices of the HA column and the usual bulk solution.

Table IV in ref. 7 summarizes values of the parameter  $\varphi'$  for phosphate ions of the buffer (pH 6.8) and the adsorption energy for one of the univalent phosphate groups on the phosphate chain of nucleoside phosphates estimated from the experimental chromatogram for a mixture of AMP, ADP, ATP and adenosine tetraphosphate. By using the value of the adsorption energy for the phosphate group estimated in ref. 7 and assumptions (1)–(3) under Theoretical (Section C), the average value of the adsorption energy for the phosphate ion of the buffer can be estimated to be 1.70–1.86 kcal/mole and, by using this value, assumption (4) under Theoretical (Section C) and the value of  $\varphi'$  estimated in ref. 7, the limiting value of  $\varphi'e^{-\varepsilon'/kT}$  when  $m$  tends to zero [see Theoretical (Section C); denoted by  $I^0$ ] is estimated to be 0.26–0.29  $M^{-1}$ . On the other hand,  $I^0$  can be evaluated by using assumption (5)

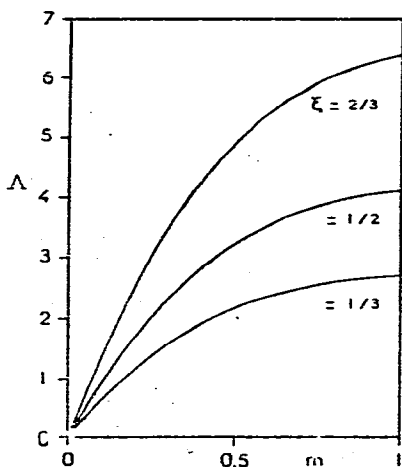


Fig. 9.  $A$  as functions of  $m$  calculated by using functions  $\gamma'(m)$  shown in Fig. 8 for three different hypothetical values of  $\xi$ . It can be seen that there are almost linear relationships between  $A$  and  $m$ , for any value of  $\xi$ , if the sodium molarity ( $m$ ) is lower than about  $10^{-1} M$ .



under Theoretical (Section C) and values of  $\varepsilon$  and  $\varphi'_{in}$  ( $\approx \varphi$ ) estimated for some different hypothetical values of  $\xi$  (Table II), the results of which are shown in the second column in Table III. It can be seen in Table III that the value of  $\Gamma^0$  estimated for the phosphate ion (see above) is closest to the value for the sodium ion obtained by assuming that  $\xi = 1/2$ . It is also close to the value for the sodium ion obtained by assuming that  $\xi = 2/3$ .

TABLE III

VALUES OF  $\Gamma^0$ ,  $\Gamma$ ,  $\beta$  AND  $\sigma$  ESTIMATED FOR SEVERAL HYPOTHETICAL VALUES OF  $\xi$ 

$\xi$	$\Gamma^0 (M^{-1})$	$\Gamma (\text{unit}^3)$	$\beta$	$\sigma^*$
1	~1.2	~3.0	~0.12	
2/3	0.49	1.21	$4.79 \cdot 10^{-2}$	1.0-1.9
1/2	0.25	0.62	$2.46 \cdot 10^{-2}$	1.3-2.7
1/3	0.08	0.20	$0.79 \cdot 10^{-2}$	1.5-4.6

\* The left- and the right-hand values are those derived by assuming the lower and the upper values of  $\beta\sigma$  in the third column in Table II, respectively.

Finally, we estimate the value of the parameter  $\beta$ , which enables us to estimate, by using the value of  $\beta\sigma$  shown in Table II, the value of  $\sigma$  that is relevant to both the geometrical configuration and the stereochemical conformation of the molecule on the crystal surface [see Theoretical (Section A)]. The parameter  $\beta$  is defined, for small loads, by eqn. A1 in Appendix I in ref. 4 or by

$$\beta = \Gamma z \cdot \frac{\delta A}{\delta V} \quad (4)$$

where  $z$  is the coordination number of P crystal sites which must be equal to 6 (see Appendix II);  $\delta A/\delta V$  is the ratio of the effective surface of HA where there are P sites to the interstitial volume in the column section, which is estimated to be  $6.6 \times 10^{-3} \text{ unit}^{-1}$ , "unit" meaning the unit length (8.77 Å) defined such that the area of the elementary surface of HA that contains a single P site would be equal to unity if it is measured in terms of this unit (see Appendix I in ref. 4);  $\Gamma$  is the ratio of the absolute activity to the concentration (number/volume) of macromolecules, which must be identical with  $\Gamma^0$ , because the actual concentration of macromolecules in the interstices of the column is very low and the value of  $\Gamma$  or  $\Gamma^0$  is independent of the type of molecules or ions. It should be noted, however, that  $\Gamma$  has dimensions of volume and that, in eqn. 4, the volume should be expressed in terms of the unit of  $(8.77 \text{ Å})^3$  (see above). As 1 M corresponds to 0.406 [number/(8.77 Å)] (see Appendix I in ref. 4), by using 0.26-0.29 M for the value of  $\Gamma^0$  obtained for phosphate ions (see above), the value of  $\Gamma$  in eqn. 4 can be estimated to be 0.64-0.71  $\text{unit}^3$ . Now, by substituting values of  $\Gamma$ ,  $z$  and  $\delta A/\delta V$  in eqn. 4,  $\beta$  is estimated to be 0.025-0.028. The parameter  $\beta$  appears to have dimensions of area, because  $\Gamma$  and  $\delta A/\delta V$  have dimensions of volume and reciprocal length, respectively, and  $z$  is a dimensionless quantity. It should be considered in eqn. 4, however, that  $\delta A/\delta V$  has dimensions of reciprocal volume, because the physical meaning of  $\delta V/\delta A$  is the interstitial volume measured in units such that the area of the elementary surface of HA that

contains a single P site would be equal to unity, which means that  $\beta$  is a dimensionless quantity. In the third column in Table III, values of  $\Gamma$  calculated from values of  $\Gamma^0$  for sodium ions obtained by assuming that  $\xi = 1, 2/3, 1/2$  and  $1/3$  are shown; in the last two columns, values of  $\beta$  and  $\sigma$  calculated by using values of  $\Gamma$  in the third column and values of  $\beta\sigma$  in the third column in Table II are shown for  $\xi = 2/3, 1/2$  and  $1/3$ , respectively. It can be seen from Table III that values of  $\beta$  calculated by assuming  $\xi = 2/3$  and  $\xi = 1/2$  are close to the value of 0.025–0.028 calculated by using the value of  $\Gamma^0$  obtained for phosphate ions (see above), which is a natural conclusion, because this value of  $\Gamma^0$  is close to the corresponding values for sodium ions obtained by assuming  $\xi = 2/3$  and  $\xi = 1/2$  (see above). It can also be seen from Table III that the values of  $\sigma$  are always slightly larger than unity; this suggests that the number of possible stereochemical conformations of the poly-L-lysine molecule on the crystal surface is close to unity (see Discussion).

## DISCUSSION

In Appendix I, the result of hydrodynamic studies on poly-L-lysine solutions carried out by Daniel and Alexandrowicz<sup>23</sup> are mentioned, which shows that low-molecular-weight poly-L-lysine molecules such as those used to obtain Fig. 1 have highly stretched conformations. It is probable that molecules of poly-L-lysine are adsorbed on arrays of P sites on crystal surfaces by conserving extended molecular conformations (see Appendix I). Further, it can be considered (see Appendix I) that, along the highly stretched chain of poly-L-lysine, there are two arrays of  $\epsilon$ -amino groups of the side-chains arranged with a minimum distance of 7.23 Å, and that every four  $\epsilon$ -amino groups on one of the two arrays, *i.e.*, every eight  $\epsilon$ -amino groups of the whole molecule, react with every three P sites on an array of P sites arranged with a minimum interdistance of 9.42 Å on the HA surface; this model is compatible with the estimation that the molecular weights of the sample range between 1500 and 8000 daltons (see the legend of Fig. 1 and Appendix I). This model would also be compatible with the value of  $\sigma$  being slightly larger than unity as estimated in Results of Calculations (see Table III); according to this model, the number of possible stereochemical conformations of the molecule on the crystal surface must virtually be equal to unity, and the number of possible geometrical configurations on the crystal surface for the  $(8n + m)$ -mer molecule, where  $n = 0, 1, 2, \dots$  and  $m = 1, 2, \dots, 8$ , can be estimated to be  $m$ , which must virtually be equal to  $\sigma$  [see Theoretical (Section A)]. As the position of the peak is influenced only slightly by the value of  $\beta\sigma$  or  $\sigma$  (see Results of Calculations), molecules with different values of  $\sigma$  would appear in the same peak if they have the same value of  $x$ . It can be estimated that the average value of  $\sigma$  is 4.5, which is slightly larger than the values estimated in Table III; this discrepancy might be due to a change in the water structure near the crystal surface that would occur when charged molecules are adsorbed on the crystal surface [*cf.*, Theoretical (Section A)] and/or the fact that the estimation of the value of  $\delta A/\delta V$  (see Results of Calculations) is not sufficiently precise.

For this type of adsorption of the molecule there are, logically, at least three possible values for the parameter  $\xi$ , *viz.*, 1, 1/2 and 1/3.  $\xi = 1$  corresponds to the case when, of three P sites under the adsorbed molecule, two sites except the one reacting with the  $\epsilon$ -amino group (see above) can react freely with sodium ions of

the buffer.  $\xi = 1/2$  corresponds to the case when one of the two crystal sites that are not reacting with the  $\epsilon$ -amino group but are under the adsorbed molecule cannot interact with the sodium ion of the buffer being blocked by the presence of the molecule. Finally,  $\xi = 1/3$  corresponds to the case when neither of these two P sites can adsorb sodium ions. In Appendix II, the distribution and the structure of P sites on the crystal surface of HA are explored on the basis of crystallographic data, according to which it is probable that P sites are arranged hexagonally with a minimum distance of 9.42 Å (between centres of sites) on the  $(\vec{a}, \vec{b})$  surface of HA and that a P site is constructed with six oxygen ions (belonging to three crystal phosphates) arranged in two triangular arrays parallel to the crystal surface. In Appendix III, the adsorption of the stretched polypeptide chain of poly-L-lysine on an array of P sites is studied by using space-filling molecular models for both poly-L-lysine and the crystal surface, the latter being constructed on the surface of the plasticine. This study suggests that the value of  $\xi$  is of the order of  $1/2$ . In Appendix IV, the chromatographic data for lysozyme discussed in ref. 4 are again discussed on the basis of several results obtained in Results of Calculations, which suggests that the value of  $\varphi$  is greater than about 7; this means that the value of  $\xi$  for poly-L-lysine is greater than about  $1/3$  (see Table II). Under Results of Calculations, it was shown, on the basis of assumptions (1)–(5) in Theoretical (Section C), that the most probable value of  $\xi$  is  $1/2$ , but that the value  $2/3$  is also probable. It follows from these estimations that the most probable value for the adsorption energy,  $\epsilon$ , for an  $\epsilon$ -amino group of poly-L-lysine on to a P crystal site is 2–2.2 kcal/mole (see Table II).

Under Results of Calculations, all calculations were carried out by assuming that the number,  $x$ , of  $\epsilon$ -amino groups of a poly-L-lysine molecule that can react with P sites is unique or that the molecule is adsorbed in the energetically most stable configuration (or configurations). More precisely, it should be considered that the geometrical configuration of the molecule on the crystal surface follows a Boltzmann distribution and that  $x$  represents the average number of adsorption groups that react with crystal sites. However, the value of 2–2.2 kcal/mole for the adsorption energy,  $\epsilon$ , obtained on the basis of the assumption of a unique value of  $x$  (see above) justifies this assumption, because values 2–2.2 kcal/mole for  $\epsilon$  correspond to values of 29–41, respectively, for the Boltzmann factor,  $e^{\epsilon/kT}$ , at 25°C. This means that the probability that the molecule is adsorbed in the energetically most stable configuration (or configurations) by using the maximum possible number of  $\epsilon$ -amino groups is approximately 29–41 times as high as the probability that it is adsorbed in different configurations, assuming that possible numbers of any geometrical configurations on the crystal surface with identical adsorption energies are about equal to one another. Hence, the molecule must virtually be adsorbed in the energetically most stable configuration (or configurations) (but see below).

It was shown (Results of Calculations) that the apparent value of  $\beta\sigma$  calculated from the pair of peaks 2 and 3 in Fig. 1 is exceptionally large (see the table in Fig. 2); this is due to the fact that the interval between peaks 2 and 3 is very narrow or that the elution molarity of peak 2 is too high, which is evident from Figs. 6 and 7. The possibility that this is experimentally fortuitous can almost be discounted, because other similar experiments have shown the same tendencies (Fig. 5b in ref. 16, Fig. 1a in ref. 8 and unpublished work by Prof. G. Bernardi). A reasonable explanation for this phenomenon can be obtained by assuming that molecules with

relatively short peptide chains (presumably with 9–16 amino residues; *cf.*, Appendices I and III) involved in peak 2 can be adsorbed on the crystal surface by using not only two  $\epsilon$ -amino groups but also more than two at the expense of the deformation of the stretched conformation of the molecule. If this is true, one cannot exclude the possibility that one of the groups that react with P sites in a deformed molecular conformation is the  $\alpha$ -amino group of the N-terminal residue. As it can be considered (see Appendix I) that the stretched conformation of the molecule is mainly due to the energetical factor, *i.e.*, the repulsive interactions among charged  $\epsilon$ -amino groups on the side-chains of the molecule, the apparent average value of the adsorption energy per amino group must decrease when there is a deformation of the molecular conformation. The decrease in the adsorption energy per amino group may also be possible if contacts of some amino groups to P sites are made incompletely in this molecular conformation. These ideas may explain qualitatively the reason why chromatographic peak 2 is displaced only slightly to a higher sodium molarity. In Fig. 1, there appears to be a small shoulder on the left-hand side of peak 2, the position of which corresponds approximately to that realized provided that molecules are adsorbed by using only two  $\epsilon$ -amino groups (see Figs. 6 and 7). This might suggest that some molecules (perhaps the smallest ones) among those involving presumably 9–16 amino residues are adsorbed by using two amino groups only. However, one cannot exclude the possibility that the occurrence of this small shoulder is experimentally fortuitous.

It was also shown (Results of Calculations) that the experimental elution volume for peak 1 is smaller than the theoretical value. A similar result was obtained in the chromatography of the mixture of nucleoside phosphates<sup>7</sup>. A qualitative explanation for these phenomena can be obtained by assuming that the conformation or the adsorption of the molecule on the crystal surface is influenced considerably by thermal motions of the molecule when it is fixed on the crystal surface with small energies and that the average energy of fixation per molecule becomes even smaller. This argument should be distinguished from that applied to the manner of adsorption of relatively large molecules (presumably with more than 16 amino residues) involved in peaks 3–9, which were used for estimations of the values of  $\epsilon$ ,  $\varphi$ ,  $\sigma$ , etc.; in this instance both the conformation and the adsorption energy of the molecule on the crystal surface can be considered to be virtually unique, because the loss of energy per molecule by the deformation of the molecular conformation must be large, and one manner of adsorption of the molecule on the HA surface must be energetically much more stable than the others (see above).

Finally, we have seen in Fig. 8 that the dependence of  $\gamma'$  on the molarity of sodium ions in the interstices of the column is different from that of the activity coefficient,  $\gamma$ , of the sodium salt in the usual aqueous solution. It can be suggested that this difference is due at least partially to the different features of the interactions among sodium ions near the HA surface from that which occurs in the usual aqueous solution\*. It is not likely that the different behaviour of  $\gamma'$  and  $\gamma$  is due to interactions

\* It might be possible that different behaviour of  $\gamma$  and  $\gamma'$  results from the fact that  $\gamma$  is the mean activity coefficient of the salt whereas  $\gamma'$  is concerned only with sodium ions. It is known, however, that the tendencies of the dependence of  $\gamma$  on the ionic strength of the solution are similar between different salts, *i.e.*,  $\gamma$  always decreases almost exponentially with increase in the square root of the ionic strength when the ionic strength is low enough (Debye–Hückel theory), while it can be seen in Fig. 8 that  $\gamma'$  decreases exponentially with increase in the ionic strength itself; this suggests that the feature of interactions among ions near the crystal surface is fundamentally different from that in the usual aqueous solution.

between sodium ions completely fixed on P sites, because 9.42 Å for the minimum distance between P sites (see Appendix II) seems to be too large for sodium ions with an ionic radius of about 1.0 Å (see ref. 24) to interact strongly enough with one another. It should be added that the exchanges of several types of cations and anions at the crystal surface of HA were studied on a kinetic basis by Pak and Bartter<sup>25</sup>; they suggested that these ions are substituted for one another at the crystal surface, including the hydration shell that is in contact with the surface, in such ways that the charge balance at the crystal surface, including the hydration shell, is conserved.

#### APPENDIX I

It is shown, by using both optical and hydrodynamic methods, that poly-L-lysine in aqueous solution undergoes a transition from a random coil to a helical conformation with an increase in pH at a pH of about 10, which is the approximate  $pK_a$  value of the  $\epsilon$ -amino group<sup>26,27</sup>. This indicates that the random coil and the helical conformations are realized when side-chains of the molecule are positively charged and neutral, respectively<sup>26</sup>, and that the molecule is in both charged and random-coil states under the chromatography conditions at pH 6.8. Several hydrodynamic properties of charged poly-L-lysine hydrochloride in aqueous solution both in the absence of the salt and in the presence of 0.01–1 M sodium chloride were investigated in detail by Daniel and Alexandrowicz<sup>23</sup>. They concluded that the effect of the ionic strength on the conformation of the molecule is small and that the frictional coefficient of the macromolecule does not depend, or depends only slightly, on the ionic strength of the solution, especially when molecules have small chain lengths; although the conformation of the molecule is called a random coil, the peptide chain of a rather small molecular weight poly-L-lysine hydrochloride (with a degree of polymerization of 50–70) is sufficiently extended in both the absence and the presence of the salt to make its frictional coefficient approximately equal to that calculated from the equation for a corresponding cylinder with a length of the repeating unit and a radius of the unit of 3.64 and about 6 Å, respectively<sup>23</sup>. Further, by interpreting the experimental results for the frictional coefficient with the Kuhn-Kuhn-Silberberg equation<sup>28</sup>, values of a statistical element length of 44 Å (or 12 monomer units) and a hydrodynamic diameter of about 8 Å were obtained<sup>23</sup>. It is probable that the poly-L-lysine hydrobromide sample with a degree of polymerization of 7–38 (see the legend of Fig. 1) used in the chromatography that resulted in Fig. 1 is highly stretched and that it is adsorbed on an array of P sites of HA conserving this molecular conformation (see below); this would be compatible with the value of  $\sigma$  being slightly larger than unity (see Table III), estimated from the chromatography (see Discussion).

The fact that the polypeptide chain of poly-L-lysine is highly stretched suggests that the region on the "molecular surface" in which a charged  $\epsilon$ -amino group can move without a considerable loss of energy is small, because the stretching of the polypeptide chain itself must be due to mutual electrostatic repulsions among  $\epsilon$ -amino groups themselves; this would mean that a close fit of the distance between  $\epsilon$ -amino groups with that between P sites of HA is necessary in order for the molecule to be fixed stably on the HA surface. According to the Corey and Pauling model<sup>29</sup>,

a fully extended polypeptide chain has a periodicity of 7.23 Å (we denote this periodicity by  $r$ ; Table AI) in the axial direction of the molecule and two side-chains orienting in opposite directions are involved in each repeating unit (*cf.*, Fig. A6). It is probable that the stretched polypeptide chain of poly-L-lysine, along both sides of which are arranged  $\epsilon$ -amino groups of the side-chains with a minimum interval of 7.23 Å (presumably with only slight fluctuations; see above) is adsorbed by using one of these two arrays of  $\epsilon$ -amino groups on one of the arrays of P sites on the crystal surface (*cf.*, Fig. A6); it is improbable that the molecule is adsorbed on the crystal surface by using both arrays of  $\epsilon$ -amino groups at the same time because, for this manner of adsorption, a considerable deformation of the molecular conformation is necessary and there is no reason why the (free) energy can be increased by this manner of adsorption (see below).

TABLE AI

RELATIONSHIPS BETWEEN THE PERIODICITY,  $r$ , FOR  $\epsilon$ -AMINO GROUPS ARRANGED ON ONE OF THE TWO ARRAYS OF THESE GROUPS ALONG THE FULLY EXTENDED POLYPEPTIDE CHAIN OF POLY-L-LYSINE AND PERIODICITIES  $q_1$ ,  $q_2$ ,  $q_3$  AND  $q_4$  FOR P SITES ON THE CRYSTAL SURFACE OF HA

(a) $v$	$rv$ (Å)	$v$	$rv$ (Å)
1	7.23	5	36.15
2	14.46	6	43.38
3	21.69	7	50.61
4	28.92	8	57.84

(b) $n$	$q_1n$ (Å)	$v$	$rv - q_1n$ (Å)
1	9.42	1	-2.19
2	18.84	3	+2.85
3	28.26	4	+0.66
4	37.68	5	-1.53
5	47.10	7	+3.51
6	56.52	8	+1.32

(c) $n$	$q_2n$ (Å)	$v$	$rv - q_2n$ (Å)
1	16.32	2	-1.86
2	32.64	5	+3.51
3	48.96	7	+1.65

(d) $n$	$q_3n$ (Å)	$v$	$rv - q_3n$ (Å)
1	24.93	3	-3.24
2	49.86	7	+0.75

(e) $n$	$q_4n$ (Å)	$v$	$rv - q_4n$ (Å)
1	33.98	5	+2.17

In Appendix II, the distribution and the structure of P sites on the crystal surface of HA are explored on the basis of crystallographic data, from which it is probable that P sites are arranged hexagonally on the crystal surface with a minimum distance of 9.42 Å. Fig. A1 illustrates schematically P sites arranged on the crystal surface and four different arrays of P sites with minimum intervals  $q_1$  (= 9.42 Å),  $q_2$  (= 16.32 Å),  $q_3$  (= 24.93 Å) and  $q_4$  (= 33.98 Å)\*. Table AI shows how the distances between  $\epsilon$ -amino groups on one of the sides of the fully extended polypeptide chain (see above) match those between P sites on the surface of HA: in part (a) are given the values of the minimum distance between  $\epsilon$ -amino groups and multiples of this value; in the second columns in parts (b), (c), (d) and (e) are given values of  $q_1$ ,  $q_2$ ,  $q_3$  and  $q_4$  (see Fig. A1) and their multiples, and in the last column in parts (b), (c), (d) and (e) are given the minimum possible differences between intervals of  $\epsilon$ -amino groups [part (a)] and those of P sites. It can be seen from Table AI that the smallest difference of 0.66 Å between the interval of  $\epsilon$ -amino groups and that of P sites occurs when poly-L-lysine is adsorbed on the array of P sites with a minimum distance of  $q_1$  or 9.42 Å and when  $\nu = 4$  and  $n = 3$ , i.e., when every four  $\epsilon$ -amino groups on one of the two arrays of these groups along the polypeptide chain react with every three P sites on the array of the minimum distance between P sites on the crystal surface [line 3 in part (b) of Table AI]. It should be noted that the slight difference between the interval of  $\epsilon$ -amino groups and that of crystal sites is due to

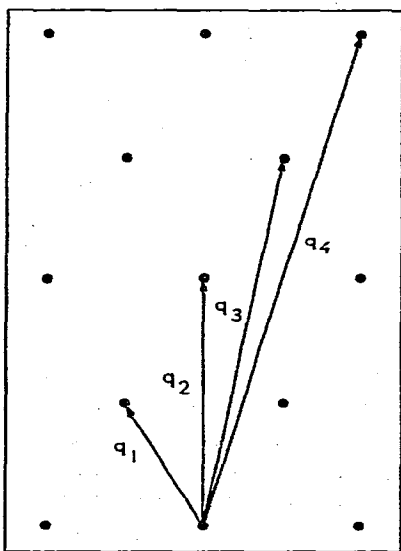


Fig. A1. Schematic representations of P sites arranged on the  $(\vec{a}, \vec{b})$  surface of HA and four different arrays of P sites with minimum intervals  $q_1$  (= 9.42 Å),  $q_2$  (= 16.32 Å),  $q_3$  (= 24.93 Å) and  $q_4$  (= 33.98 Å).

\* In ref. 4, it is mentioned that  $|\vec{a}| \cong q_1 = 9.432$  Å, which is cited from ref. 11. In this paper, we use the value 9.42 Å for  $|\vec{a}|$  obtained on the basis of a more precise crystallographic study of HA in ref. 12.

the fact that the former is slightly larger than the latter, which must be a better condition for the adsorption of the molecule on to the crystal surface than if the former interval was smaller than the latter, because the fully stretched molecule can contract but cannot extend any more. Further, Table AI shows (1) that, in order for a larger proportion than one quarter of the  $\epsilon$ -amino groups on one of the two arrays of these groups along the polypeptide chain to interact with P sites, *i.e.*, in order for the value of  $\nu$  to be smaller than 4, the difference between the interval of  $\epsilon$ -amino groups and that of P sites has to be much larger than 0.66 Å or it has to be 1.86–3.24 Å, and (2) that, in order for the difference between the interval of adsorption groups and crystal sites to be smaller than 0.66 Å, the value of  $\nu$  has to be greater than 5, *i.e.*, the proportion of  $\epsilon$ -amino groups that can react with P sites has to be less than one fifth of those existing on one of the two arrays of the side-chains of the polypeptide chain, because the adsorption of the molecule has to occur on the array of P sites with a minimum distance larger than  $q_4$  or 33.98 Å. This indicates that the manner of adsorption of poly-L-lysine such that every four  $\epsilon$ -amino groups on one of the two arrays of the side-chains of the polypeptide chain interact with every three P sites arranged on an array of P sites with a minimum distance of 9.42 Å is energetically the most stable, assuming (a) that there is virtually no increase in the energy of interaction between an  $\epsilon$ -amino group and a P site if the difference between the interval of  $\epsilon$ -amino groups and that of P sites decreases further from 0.66 Å, but (b) that there is a considerable loss of energy if the difference between the two intervals exceeds 1.86 Å, which are reasonable assumptions.

This model for the manner of adsorption of poly-L-lysine on the surface of HA is strongly supported by the following result of a simple calculation. As the degree of polymerization of the poly-L-lysine sample used to obtain the chromatogram in Fig. 1 is estimated to range between 7 and 38 (see the legend of Fig. 1), by assuming that every eight  $\epsilon$ -amino groups of the whole molecule interact with P sites, the numbers of  $\epsilon$ -amino groups per molecule that interact with P sites or the value of  $x$  can be estimated to range between 7/8 and 38/8, *i.e.*, between about 1 and 5; these  $x$  values correspond, according to the interpretation of the chromatogram made under Theoretical (Section C), to the  $x$  values for molecules involved in peaks 1–5, which occupy most of the chromatogram in Fig. 1.

Finally, we see no reason why the (free) energy can be increased provided that molecules are adsorbed on the crystal surfaces by taking conformations different to a stretched conformation because, firstly, deformation of the molecular conformation from the stretched state must accompany a decrease in energy because of an increase in repulsive interactions among charged  $\epsilon$ -amino groups (see above), and secondly, the range of the values of  $x$  estimated from the experimental chromatogram can be explained by assuming the stretched molecular conformation which should be the most stable (see above, but see also Discussion for the manners of adsorption of molecules with very short peptide chains presumably with less than 17 amino residues).

## APPENDIX II

It would be reasonable, in general, to consider that mechanisms of the adsorption of both free ions and adsorption groups of macromolecules on to crystal



surfaces resemble the first step of the epitaxial growth of the crystal, where epitaxy consists in the growth of one crystal, in one or more particular orientations, on a substrate of another, with a near geometrical fit between the respective networks that are in contact<sup>30</sup>. In the Introduction, it was mentioned that both free cations of the buffer and basic groups of basic macromolecules must be adsorbed on the flat crystal surface of HA which is parallel to  $(\vec{a}, \vec{b})$  planes of unit cells. It is probable that both cations and basic groups are adsorbed, if not exactly, on positions of the crystal surface where calcium ions should be coordinated, provided that the crystal structure extends over the actual surface. This idea is supported by the fact that, at least in the interior of the crystal structure,  $\text{Ca}^{2+}$  ions can be partially replaced with ions such as  $\text{Na}^+$ ,  $\text{K}^+$  and  $\text{Pb}^{2+}$  (ref. 31). It is known that there are two types of calcium ions, called  $\text{Ca}_I$  and  $\text{Ca}_{II}$  ions, in the interior of the HA structure, classified according to the environments in which the ions are arranged\*, which are shown in Figs. A2 and A3, respectively. Therefore, there are two types of possible positions of P sites on the crystal surface of HA.

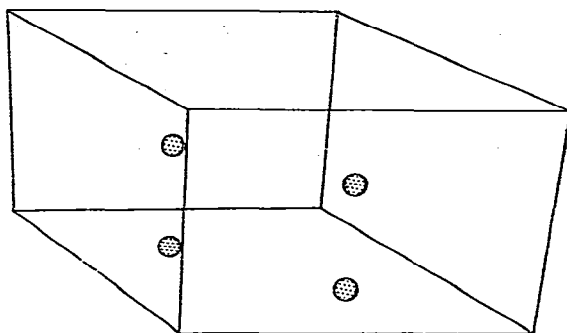


Fig. A2. Perspective view of  $\text{Ca}_I$  ions. The outline of the unit cell is also shown, where  $\vec{a}$  is horizontally directed to the right in the plane of the paper,  $\vec{b}$  is directed into the paper and  $\vec{c}$  is vertical and upwards. The ions are shown at a small size in comparison with the size of the unit cell. It can be seen that there are two columns of  $\text{Ca}_I$  ions per unit cell along two three-fold rotational symmetry axes, and that each column is constituted of two  $\text{Ca}_I$  ions occurring at  $z = 0.00$  and  $z = 0.50$  (nearly but not precisely at  $z = 0$  and  $z = 1/2$ , respectively). (Reproduced from ref. 13 with the permission of Prof. R. A. Young).

We examine first the possibility that a  $\text{Ca}_{II}$  position (devoid of calcium ions) on the crystal surface corresponds to a P site. As can be seen in Fig. A3, there are a pair of triangular arrays of  $\text{Ca}_{II}$  ions per unit cell centred on each edge ( $6_3$  axis) of the cell, which lie on two mirror planes [parallel to the  $(\vec{a}, \vec{b})$  plane] being at levels of  $z = 1/4$  and  $z = 3/4$ , and they are inserted by two parallel triangles of oxygen ions ( $\text{O}_{III}$  ions; not shown in the figure) being at  $z = 0.07$  and  $z = 0.43$  and at  $z = 0.57$  and  $z = 0.93$ . As six  $\text{O}_{III}$  ions inserting one of the  $\text{Ca}_{II}$  triangles belong to three crystal phosphates, the phosphorus atoms of which are at the same level as that of the  $\text{Ca}_{II}$  triangle itself, it is impossible for  $\text{Ca}_{II}$  ions to be exposed to the medium at the crystal surface parallel to  $(\vec{a}, \vec{b})$  planes of unit cells. Therefore, it is also im-

\* For details of the crystallography of HA, see refs. 11-13.

possible for "Ca<sub>II</sub> positions devoid of calcium ions", if they exist, to be exposed to the medium at the  $(\vec{a}, \vec{b})$  crystal surface. However, as Ca<sub>II</sub> triangles are smaller than O<sub>III</sub> triangles and as they are both centred on the same 6<sub>3</sub> axes of the unit cells (see Fig. A3), it might be possible that, although Ca<sub>II</sub> positions are buried in "holes" made by O<sub>III</sub> triangles at the crystal surface, they are partially exposed to the medium. Therefore, if they are devoid of calcium ions, they might constitute adsorbing sites; this is improbable, however, because, there appears to be no reason why only Ca<sub>II</sub> positions at the crystal surface that are coordinated by six oxygen ions in the same manner as for Ca<sub>II</sub> positions in the interior of the crystal should be devoid of calcium ions. Even if only Ca<sub>II</sub> positions at the crystal surface are devoid of calcium ions (although this is an improbable assumption), it is improbable that they correspond to P sites for the following reason: if Ca<sub>II</sub> positions on the crystal surface correspond to P sites, there must be three P sites per unit crystal cell or parallelogram made by vectors  $\vec{a}$  and  $\vec{b}$  where  $|\vec{a}| = |\vec{b}| = 9.42 \text{ \AA}$ , from which it can be estimated that the number of P sites that are covered by a molecule of lysozyme adsorbed on the crystal surface is of the order of 30, assuming that lysozyme is represented by a prolate spheroid of dimensions  $45 \times 30 \times 30 \text{ \AA}$ , that the adsorption is such that the maximum molecular surface is brought into contact with the crystal and that most of the sites under the adsorbed molecule are covered<sup>4</sup>. On the other hand, the most probable numbers of P sites covered by an adsorbed lysozyme are estimated to be 4–8 or even 6–7 from the analysis of the chromatographic behaviour of lysozyme (see Appendix IV), which could be explained only by assuming that there is only one P site per parallelogram of vectors  $\vec{a}$  and  $\vec{b}^*$ .

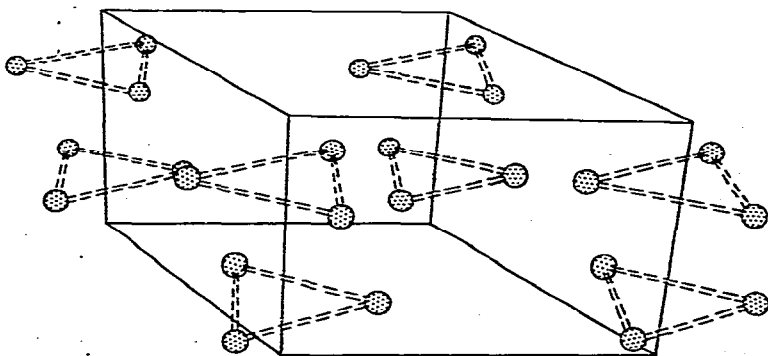


Fig. A3. As Fig. A2, but for Ca<sub>II</sub> ions. It can be seen that there are a pair of triangular arrays of Ca<sub>II</sub> ions centred on each edge (6<sub>3</sub> axis) of the unit cell, or that there are a pair of triangular arrays of Ca<sub>II</sub> ions per unit cell, which lie on two mirror planes [parallel to the  $(\vec{a}, \vec{b})$  plane] being at levels of  $z = 1/4$  and  $z = 3/4$ , respectively. (Reproduced from ref. 13 with the permission of Prof. R. A. Young).

\* It may be possible that they are only some of the sites under the adsorbed molecule that are covered by the molecule, as with poly-L-lysine (see Appendix III). Even taking into account this possibility, the assumption that there is only one P site per parallelogram of vectors  $\vec{a}$  and  $\vec{b}$  seems to be most reasonable in order to explain the very small number of P sites covered by an adsorbed lysozyme estimated experimentally. In fact, this number would suggest that some of P sites (arranged at every 9.42 Å) under the adsorbed molecule are not covered by the molecule.

Now, we examine the alternative possibility that it is a  $\text{Ca}_I$  position (devoid of calcium ions) that corresponds to a P site. As can be seen in Fig. A2, there are two columns of  $\text{Ca}_I$  ions per unit cell along two three-fold rotational symmetric axes, and each column consists of two  $\text{Ca}_I$  ions occurring at  $z = 0.00$  and  $z = 0.50$  (nearly but not precisely, at  $z = 0$  and  $z = 1/2$ , respectively). Each  $\text{Ca}_I$  ion is coordinated by nine oxygen ions in three triangular arrays parallel to the  $(\vec{a}, \vec{b})$  plane, centred on the  $\text{Ca}_I$  column itself, and one above (along positive  $\vec{c}$ ), one below and one at nearly the same level (*cf.*, Figs. A4 and A5). Fig. A4 illustrates schematically a projected view of a column of unit crystal cells on an  $(\vec{a}, \vec{c})$  or a  $(\vec{b}, \vec{c})$  plane, in which the dots and thick horizontal lines represent  $\text{Ca}_I$  ions and oxygen triangles, respectively; thick lines at  $z = 0.07$ ,  $z = 0.43$ , etc., which represent triangles of  $\text{O}_{III}$  ions, are drawn long in order to emphasize that these triangles are larger than the other two types of triangles of  $\text{O}_I$  and  $\text{O}_{II}$  ions which are represented by thick lines inserted between two dots of  $\text{Ca}_I$  ions and those inserted between two thick lines of  $\text{O}_{III}$  ions, respectively. Projected views, on an  $(\vec{a}, \vec{b})$  plane, of three triangles of  $\text{O}_I$ ,  $\text{O}_{II}$  and  $\text{O}_{III}$  ions at  $z = 3/4$ ,  $z = 3/4$  and  $z = 0.93$  are drawn in Fig. A5, from which it can be understood that three successive  $\text{O}_{III}$ ,  $\text{O}_{II}$  and  $\text{O}_{III}$  triangles (the levels of which are relatively close to one another; see Fig. A4) belong to three crystal phosphates, the phosphorus atoms of which are at the same level as that of the  $\text{O}_{II}$  triangle itself of this series; this excludes the possibility that a plane inserted between  $\text{O}_{II}$  and  $\text{O}_{III}$

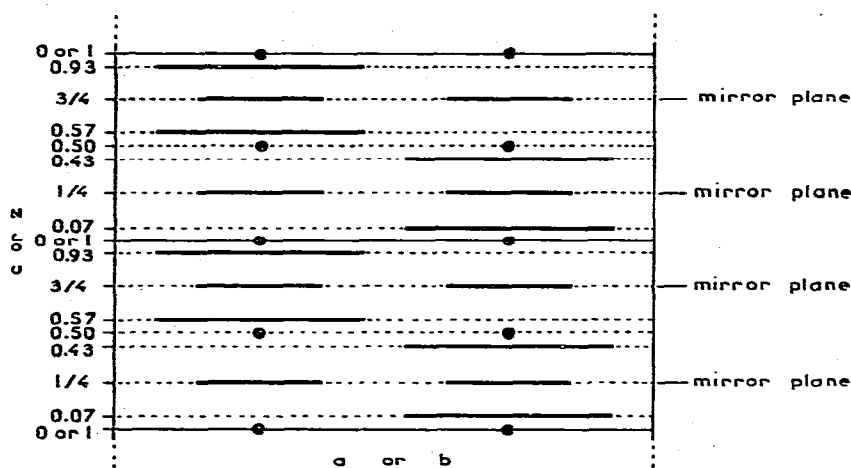


Fig. A4. Schematic representation of a projected view of a column of HA unit cells on an  $(\vec{a}, \vec{c})$  or a  $(\vec{b}, \vec{c})$  plane. The dots and thick horizontal lines represent  $\text{Ca}_I$  ions and oxygen triangles, respectively. [The other components of the crystal: phosphorus at mirror planes,  $\text{Ca}_{II}$  ions at mirror planes near  $6_3$  axes (see Fig. A3) and hydroxyl ions near mirror planes at  $6_3$  axes are not shown]. Thick lines at  $z = 0.07$ ,  $z = 0.43$ , etc., which represent triangles of  $\text{O}_{III}$  ions, are drawn long in order to emphasize that these triangles are larger than the other two types of triangles of  $\text{O}_I$  and  $\text{O}_{II}$  ions, which are represented by thick lines inserted between two dots of  $\text{Ca}_I$  ions and those inserted between two thick lines of  $\text{O}_{III}$  ions, respectively. Three successive  $\text{O}_{III}$ ,  $\text{O}_{II}$  and  $\text{O}_{III}$  triangles, the levels of which are relatively close to one another, belong to three crystal phosphates, the phosphorus atoms of which are at the same level as that of the  $\text{O}_{II}$  triangle itself of this series; this excludes the possibility that a plane inserted between  $\text{O}_{II}$  and  $\text{O}_{III}$  triangles appears on the crystal surface.

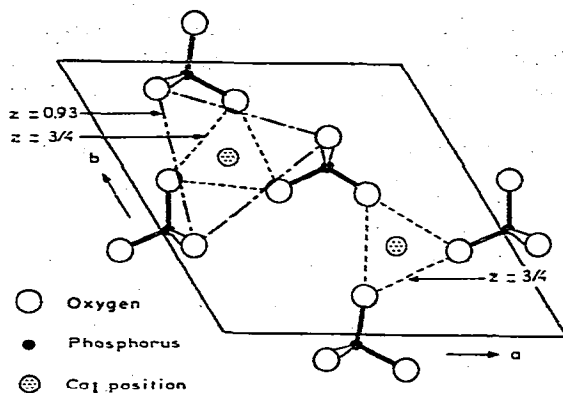


Fig. A5. Deduced structure of the  $(\vec{a}, \vec{b})$  surface of HA. Crystal phosphates and two  $\text{Ca}_1$  positions appearing on the  $(\vec{a}, \vec{b})$  surface of HA are shown at a small size in comparison with the outlined unit cell. It can be considered that both the cation of the buffer and the positively charged group of the macromolecule are adsorbed mainly at or near the left-hand  $\text{Ca}_1$  position coordinated by three  $\text{O}_{II}$  and three  $\text{O}_{III}$  ions that constitute triangular arrays at  $z = 3/4$  and  $z = 0.93$ , respectively, and that this position corresponds to a P site. It is probable that the cation and the positively charged group of the macromolecule are also adsorbed weakly at or near the right-hand  $\text{Ca}_1$  position coordinated by three  $\text{O}_I$  ions at  $z = 3/4$ . (Reproduced with modifications from Fig. 2c in ref. 13 with the permission of Prof. R. A. Young).

triangles appears on the crystal surface. Thus, it must be a plane between two  $\text{O}_{III}$  triangles centered on neighbouring  $\text{Ca}_1$  columns or the level of  $\text{Ca}_1$  positions that appears on the crystal surface (see Fig. A4). Therefore,  $\text{Ca}_1$  positions exposed to the medium at the crystal surface would be expected to adsorb both cations of the buffer and positively charged groups of macromolecules, if they are devoid of calcium ions; the latter condition is probable because two types of  $\text{Ca}_1$  positions at the crystal surface are coordinated by only six oxygen ions (in two triangular arrays) and by only three (in a single triangular array) (see Figs. A4 and A5); in contrast to a  $\text{Ca}_1$  position in the interior of the crystal, which is coordinated by nine oxygen ions in three triangular arrays (see Fig. A4), and whether or not  $\text{Ca}_1$  positions at the crystal surface are occupied by calcium ions does not seem to be important for the cooperativity of the crystal structure as a whole.

It is probable that  $\text{Ca}_1$  positions coordinated by six oxygen ions adsorb both free cations and adsorption groups of macromolecules with much higher probabilities than those coordinated by three oxygen ions because, firstly, the probability that both free ions and adsorption groups of macromolecules are adsorbed on to  $\text{Ca}_1$  positions coordinated by six oxygen ions must be higher than the probability that they are adsorbed on positions coordinated by three oxygen ions, for energetic reasons. Secondly, the chromatographic results with lysozyme could be explained most satisfactorily by assuming that there is only one adsorbing site per parallelogram made by vectors  $\vec{a}$  and  $\vec{b}$  (see above) and this is possible only when one of the two types of  $\text{Ca}_1$  positions is a practical adsorbing site. Thirdly, it was shown in ref. 14 that the  $\text{HPO}_4^{2-}$  ion adsorbed on a hydroxyl position (C site) of HA should have three appropriate calcium to oxygen distances of 2.39–2.63 Å and a hydrogen bond length of 2.46 Å and, in Part IV<sup>7</sup>, that the energy of the adsorption for a univalent

phosphate group on the polyphosphate chain of nucleoside phosphates (which should also be adsorbed on to C sites) should be 0.9–1 kcal/mole (see Introduction)\*. Under Results of Calculations, the adsorption energy for an  $\epsilon$ -amino group of poly-L-lysine on to a P site was estimated to be 2–2.2 kcal/mole, in spite of the fact that this adsorption group has only a single charge, which seems to be possible only when the adsorption group is coordinated by six oxygen ions. Fourthly, it is improbable that  $\text{Ca}_I$  positions coordinated by six oxygen ions are almost always occupied by calcium ions and that only those coordinated by three oxygen ions are available for the adsorption of both cations of the buffer and adsorption groups of macromolecules because, even if the energy for the occupation of a  $\text{Ca}_I$  position by a calcium ion is higher than that for occupation by an adsorption group of the macromolecule, the energy per molecule with several active adsorption groups would exceed the energy per calcium ion, and  $\text{Ca}_I$  positions would be occupied by adsorption groups of macromolecules rather than calcium ions. Similarly, if the concentration of competing cations in solution is much higher than that of calcium ions (which is the usual practice),  $\text{Ca}_I$  positions must be occupied by competing cations rather than calcium ions. Finally, the possibility that one of the two types of  $\text{Ca}_I$  positions is occupied only by competing cations and that the others are occupied only by adsorption groups of macromolecules can almost be excluded from the study of the adsorption of poly-L-lysine on the crystal surface performed by using space-filling models (see Appendix III).

Hence, it is probable that a  $\text{Ca}_I$  position coordinated by six oxygen ions (three  $\text{O}_{II}$  and three  $\text{O}_{III}$  ions) corresponds to a P site, the detailed structure of which is shown in both Figs. A5 and A6.

### APPENDIX III

In Appendix II, it was mentioned that P sites must be arranged hexagonally with a minimum distance of 9.42 Å on the  $(\vec{a}, \vec{b})$  surfaces of HA and that a P site must be constructed with six oxygen ions (three  $\text{O}_{II}$  and three  $\text{O}_{III}$  ions) belonging to three crystal phosphates. In Appendix I, it was mentioned that the polypeptide chain of poly-L-lysine must be highly stretched under the experimental conditions

\* It can be considered that a C site is constructed with two  $\text{Ca}_{II}$  ions (at the same  $z$  surrounding the same  $6_3$  axis; cf., Fig. A3) or two  $\text{Ca}_{II}$  ions plus an oxygen ion of the crystal phosphate when the adsorbed phosphate or the phosphate group of the adsorbed polyphosphate contains a hydrogen atom. In Fig. 1 in ref. 14 (or Fig. 1 in ref. 7), the manner of fixation of an  $\text{HPO}_4^{2-}$  ion on to a hydroxyl position (a C site) of the HA part of octacalcium phosphate is shown, where it can be seen that an oxygen (No. 35) of the phosphate ion interacts with two  $\text{Ca}_{II}$  ions (Nos. 6 and 8) of HA with distances of 2.63 and 2.37 Å, respectively; another oxygen (No. 38) of the phosphate ion interacts with  $\text{Ca}_{II}$  ion (No. 6) of HA with a distance of 2.39 Å, and another oxygen (No. 36) of the phosphate ion interacts with an  $\text{O}_{III}$  ion (No. 20) of HA through the hydrogen atom of the phosphate ion constituting a hydrogen bond length of 2.46 Å. It should be noted that, in Fig. 1 in ref. 14, atomic positions in the HA cell are the mirror image of those in Fig. A5 or that, in the former figure, atomic positions are projected from under the plane of the paper of the latter figure. It should also be noted that coordinates of the atoms determined for the HA part of octacalcium phosphate<sup>22</sup> are slightly different from those determined very precisely for the HA crystal<sup>12</sup>; therefore, the distances between the oxygen and hydrogen atoms of the phosphate ion and some crystal ions estimated above would be slightly different in adsorption of the phosphate ion on to the HA crystal surface in the chromatographic experiment.

and that it must be adsorbed on the surface of HA in such a manner that every four  $\epsilon$ -amino groups on one of the two arrays of these groups along the stretched polypeptide chain, where the minimum distance between these groups is 7.23 Å, must react with every three P sites on an array of P sites arranged with a minimum distance of 9.42 Å on the crystal surface. For this type of adsorption, there are, logically, at least three possible values of the parameter  $\xi$ , viz., 1, 1/2 and 1/3 (see Discussion).

Fig. A6a shows a photograph of space-filling models of poly-L-lysine undecamer and two sodium ions adsorbed on the model surface of HA, which was constructed on the surface of the plasticine also by using space-filling models of phosphate ions. Parallelograms on the surface of the plasticine show outlines of crystal unit cells projected on an  $(\vec{a}, \vec{b})$  plane. On the left-hand side of the photograph, a free P site constructed with three  $O_{II}$  and three  $O_{III}$  ions and a presumably weak adsorbing site constructed with three  $O_I$  ions can be seen (see Appendix II and Fig. A5). It can also be seen that a molecule of poly-L-lysine that is extended almost completely not only in the axial direction, the N-terminal being on the left-hand side, but also in the direction perpendicular to it\*, is adsorbed by using two  $\epsilon$ -amino groups of the side-chains belonging to the second amino residues from the N- and the C-terminal residues of the peptide chain on to every three P sites. For the conformation of the  $\epsilon$ -amino group reacting with a P site, it is assumed that the plane defined by the three hydrogens of the tetrahedron of the charged or the protonated primary amine is parallel to the triangular arrays of both  $O_{II}$  and  $O_{III}$  ions of crystal phosphates and that each hydrogen of the primary amine is superposed on each  $O_{II}$  ion and inserted by two  $O_{III}$  ions; in this manner of adsorption, each hydrogen of the  $\epsilon$ -amino group can be kept in contact with one  $O_{II}$  and two  $O_{III}$  ions with reasonable distances of about 2.5 Å (see Fig. A6a). One could not, however, preclude the possibility that the triangle of the three hydrogens of the protonated primary amine is superposed on the triangle of the  $O_{II}$  ions with a displacement of 60° to each other. It should be noted in Fig. A6 that the molecule is brought into contact with the HA surface through the array of five  $\epsilon$ -amino groups and not through the opposite array of six  $\epsilon$ -amino groups, which is only for the sake of convenience. It is evident that, if the molecule is adsorbed through this array, it can be adsorbed in two different configurations; therefore, there is a total of three possible geometrical configurations on the HA surface for the stretched undecamer molecule (*cf.*, Discussion).

Possible conformations for three  $\epsilon$ -amino groups of the molecule that are in contact with the crystal surface but are not superposed on P sites (see Fig. A6a) appear to be limited, being blocked by the existences of protruding  $O_{III}$  ions on the crystal surface, which can be understood from Fig. A6b, where three intermediate side-chains in contact with the HA surface of the model molecule in Fig. A6a are shown from the rear. It can be seen in Fig. A6b that a hydrogen of the  $\epsilon$ -amino

\* This is an assumption, but it is reasonable because the average distance among charged  $\epsilon$ -amino groups is maximal in this conformation. Under Discussion, it was suggested that poly-L-lysine with 9-16 amino residues is adsorbed on the crystal surface not only in the stretched conformation (in the axial direction) but also in a deformed conformation or conformations by using more than two  $\epsilon$ -amino groups. Here, we consider only the stretched conformation for the undecamer model of poly-L-lysine, however, because our purpose is to understand the manner of adsorption of molecules with higher molecular weights by using this model.

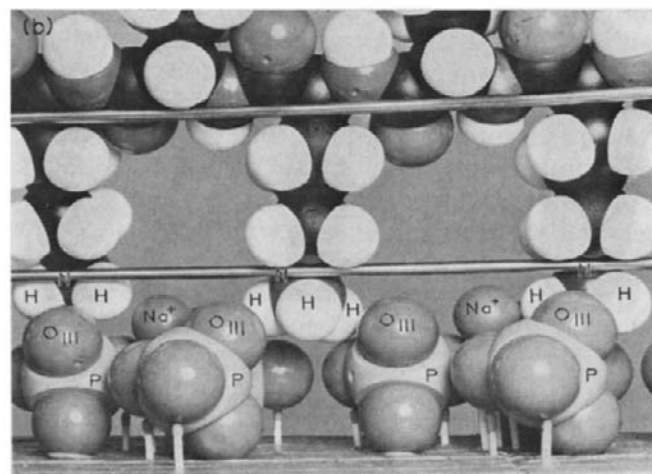
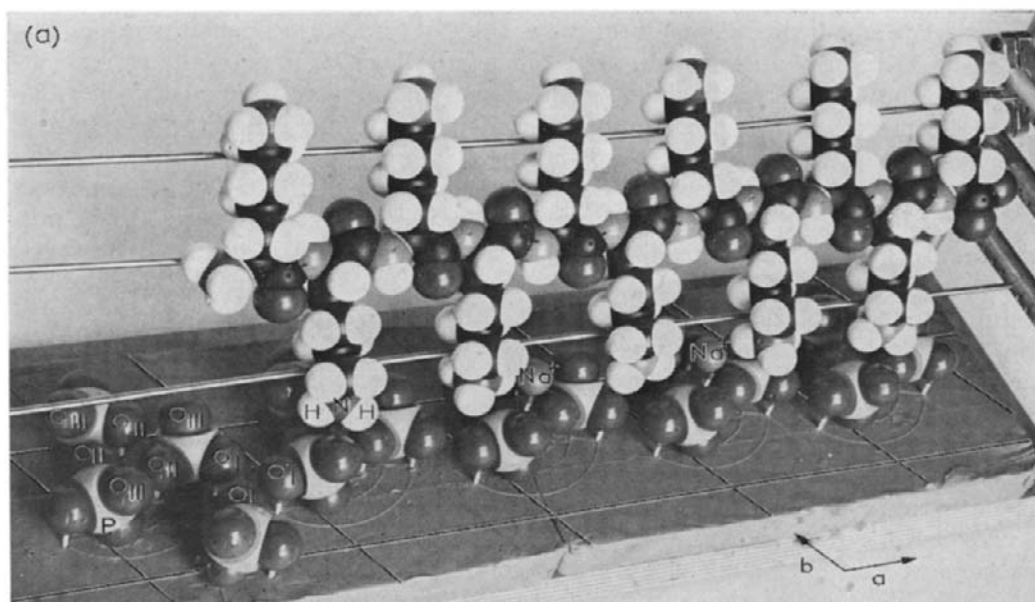


Fig. A6. (a) Photograph of space-filling models of a poly-L-lysine undecamer and two sodium ions adsorbed on the model surface of HA which is constructed on the surface of the plasticine also by using space-filling models of phosphates. Parallelograms on the surface on the plasticine show outlines of crystal unit cells projected on an  $(\vec{a}, \vec{b})$  plane. On the left-hand side, a free P site constructed with three  $O_{II}$  and three  $O_{III}$  ions and a presumably weak adsorbing site constructed with three  $O_I$  ions can be seen (*cf.*, Fig. A5). It can also be seen that a molecule of poly-L-lysine which is almost completely extended not only in the axial direction, the N-terminal being on the left-hand side, but also in the direction perpendicular to it is adsorbed by using two  $\epsilon$ -amino groups of the side-chains belonging to the second amino residues from the N- and C-terminal ones of the peptide chain, respectively, onto every three P sites. (b) Photograph of three intermediate side-chains in contact with the HA surface but not superposed on P sites of the model molecule shown in (a), taken from the rear side, and two sodium ions adsorbed on P sites.

group of the right-hand side-chain intrudes slightly into the triangular array of  $O_{III}$  ions of crystal phosphates in order to avoid protruding  $O_{III}$  ions on the crystal surface, while the left-hand side-chain is slightly raised in order to avoid another  $O_{III}$  ion; the conformation of the intermediate  $\epsilon$ -amino group seems to be less limited. In spite of the presences of these side-chains of the molecule, adsorption of competing or sodium ions on to both of  $Ca_I$  positions (see Appendix II), which are under the adsorbed molecule but are not superposed by  $\epsilon$ -amino groups, seems to be possible (see Figs. A6a and b) and the value of  $\xi$  seems to be close to unity. However, the position of the hydrogen of the right-hand  $\epsilon$ -amino group in Fig. A6b or the  $\epsilon$ -amino group of the left-hand side-chain of the intermediate three side-chains in contact with the HA surface in Fig. A6a is so close to the  $Ca_I$  position of the crystal that it might prevent the adsorption of the sodium ion on to this  $Ca_I$  position, whereas it does seem unlikely that the adsorption of the sodium ion on to the left-hand  $Ca_I$  position in Fig. A7b is prevented; this would mean that the value of  $\xi$  is close to 1/2. Further, it was shown by Bernardi (unpublished work) that an almost identical chromatogram for the low-molecular-weight poly-L-lysine sample can be obtained by using a  $K^+$  system instead of the  $Na^+$  system, which would mean that potassium ions are adsorbed on the crystal surface in a similar manner to sodium ions in relation to the position of the adsorbed macromolecule. As the ionic radius of the potassium ion (1.3 Å) is larger than that of the sodium ion (1.0 Å)<sup>24</sup>, it might be very difficult for the potassium ion to be adsorbed on to the right-hand  $Ca_I$  position in Fig. A6b. One cannot, however, exclude the possibility such that adsorption of sodium or potassium ions on to both or one of the  $Ca_I$  positions is partially hindered by side-chains of poly-L-lysine, and/or that  $\epsilon$ -amino groups of the molecule interact slightly with the surface of HA even if they are not superposed completely on P sites, which would contribute slightly to the (apparent) value of  $\xi$ . Taking into account all of these factors, the probable value of  $\xi$  seems to be of the order of 1/2.

Finally, the possibility that one of the two types of  $Ca_I$  positions on the crystal surface that are coordinated by six and three oxygen ions, respectively, react with adsorption groups of macromolecules and that the other  $Ca_I$  positions react only with competing ions (which was considered in Appendix II) can almost be excluded by examining Fig. A6a; it is evident that all  $Ca_I$  positions coordinated by only three  $O_I$  ions are acceptable to sodium ions, even if the maximum number of  $Ca_I$  positions coordinated by three  $O_{II}$  and three  $O_{III}$  ions are occupied by macromolecules and *vice versa*, which means that there is no competition between macromolecules and sodium ions for adsorption on to the crystal surface if they are adsorbed on to different types of  $Ca_I$  positions.

#### APPENDIX IV

In an earlier paper<sup>4</sup>, chromatographic data for lysozyme and cytochrome *c* were plotted on the  $[m_{elut(K^+)}, \ln S_{(K^+)}]$  plane, and values of parameters such as  $x'$  and  $\ln q$  were estimated for these basic molecules on the basis of the theory developed in the same paper<sup>4</sup> and by assuming, in most calculations, that the activity coefficient of  $K^+$  ions in the interstices of the column is equal to the mean activity coefficient of potassium chloride measured in the usual aqueous solution. Under Results of Calculations, it was shown, however, that the dependence of the activity of sodium



ions on the concentration in the column interstices is different from that measured for sodium chloride in the usual aqueous solution, probably owing to particular interactions among sodium ions occurring near the crystal surface of HA (see Discussion); the "activity coefficient",  $\gamma'$ , of sodium ions in the column interstices varies less with an increase in the cation concentration,  $m$ , than does the activity coefficient,  $\gamma$ , of sodium chloride or potassium chloride in the usual aqueous solution in the range of small  $m$  values (see Fig. 8), and as the result of the mild dependence of  $\gamma'$  on  $m$ , the parameter  $\lambda$  increases almost linearly with an increase in  $m$  when  $m$  is small (see Fig. 9). Here, by assuming that the dependence of  $\lambda$  on  $m$  for potassium ions

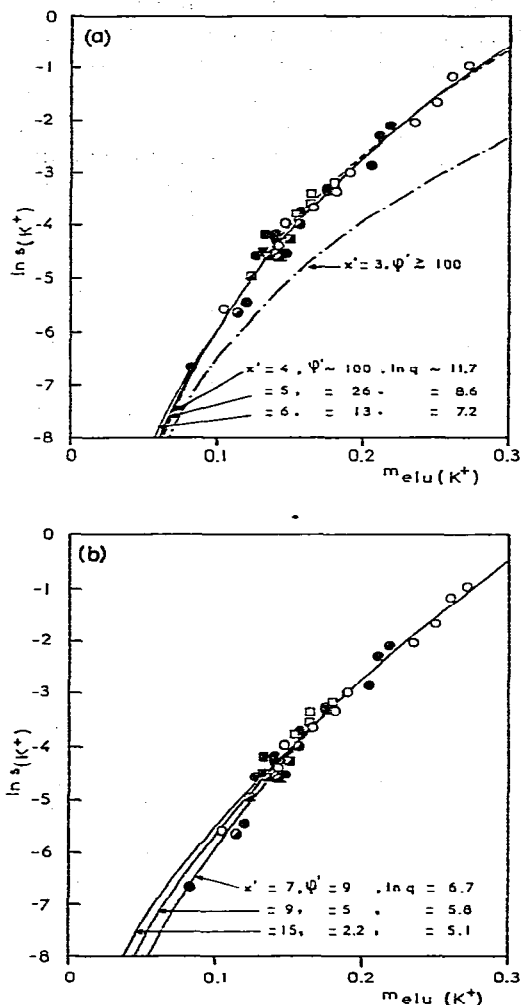


Fig. A7. (a) Points: experimental plots of  $\ln s_{(K^+)}$  versus  $m_{elu}(K^+)$  for lysozyme reproduced from Fig. 2b, c or e in ref. 4. The curves are theoretical, obtained by giving values of 3-6 to  $x'$ . It can be seen that good fits with the experimental results can be obtained only when  $x' \geq 4$ . (b) As (a), but the theoretical curves were obtained by giving values of 7-15 to  $x'$ . It can be seen that good fits with the experimental values can be obtained only when  $x' = 7$ .

is virtually the same as that for sodium ions\*, chromatographic data for lysozyme and cytochrome *c* shown in Fig. 2b, d and e and Fig. 4 in ref. 4, respectively, are again analysed on the basis of eqn. 15 in ref. 4, and more precise values of  $x'$ ,  $\ln q$ , etc., for these molecules are estimated.

The points in Fig. A7a and b are experimental plots of  $\ln s_{(K^+)}$  versus  $m_{\text{elu}(K^+)}$  (for definitions of these parameters, see ref. 4) for lysozyme reproduced from Fig. 2b, d or e in ref. 4; the curves are theoretical, calculated by using eqn. 15 in ref. 4, assuming a linear relationship between  $\Delta$  and  $m$  (see above) and giving values of 3-7, 9 and 15 for  $x'$  and values that give the best fits with the experimental results for  $\varphi'$  and  $\ln q$  (except when  $x' = 3$ ; see below)\*\*. It can be seen in Fig. A7a and b that, when  $x' \geq 9$ , the theoretical curves are less curved than the experimental result; when  $4 \leq x' \leq 7$ , good fits between the theoretical and experimental results are obtained, and when  $x' = 3$  the average slope of the theoretical curve is almost constant and is always less than that of the experimental result provided that  $\varphi' \geq 100$ . If  $\varphi' \leq 100$ , the average slope of the curve becomes even smaller, and no good fits with the experimental values can be obtained when  $x' = 3$ . In the first three columns in Table AII are summarized the best values of  $x'$ ,  $\varphi'$  and  $\ln q$ ; it should be noted that best values (10-15) for  $\varphi$  obtained from the experiment with poly-L-lysine (see Results of Calculations and Discussion) are involved in the region of the best values of  $\varphi'$  obtained from a different type of experiment for lysozyme. In columns 6, 8 and 9 in Table AII are given values of  $x\varepsilon/kT$ ,  $x$  and  $\xi$  for lysozyme estimated for two most reasonable values of  $\varphi'$  (13 and 9), which are slightly smaller than best values (15 and 10) for  $\varphi$  (see above). In fact, by taking into account the fact that the linear dependence of  $\Delta$  on the molarity,  $m$ , becomes slightly invalid with increase in  $m$  in the range of the experiment with lysozyme, *i.e.*, in the range  $0 \leq m \leq 0.3$

TABLE AII  
PARAMETERS ESTIMATED FOR LYSOZYME

$x'$	$\varphi'$	$\ln q$	$\beta$ (assumed)	$\sigma$ (assumed)	$x\varepsilon/kT$	$\varepsilon$ (assumed) (kcal/mole)	$x$	$\xi$
4	$\sim 100$	$\sim 11.7$						
5	$26 \pm 2$	8.6						
6	$13 \pm 2$	7.2	$4.79 \cdot 10^{-2}$	1	10.2	2.03	3.0	0.50
				2	9.6		2.8	0.47
				4	8.9		2.6	0.43
				10	7.9		2.3	0.38
7	$9 \pm 1$	6.7	$2.46 \cdot 10^{-2}$	1	10.4	2.20	2.8	0.40
				2	9.7		2.6	0.37
				4	9.0		2.4	0.34
				10	8.1		2.2	0.31
8	$7 \pm 1$	6.5						

\* This is a reasonable assumption, because almost identical chromatograms for the low-molecular-weight poly-L-lysine sample are obtained by using  $\text{Na}^+$  and  $\text{K}^+$  systems (Bernardi, unpublished data; see Appendix III).

\*\* It can be understood from eqn. 15 in ref. 4 that the shape of the curve depends on  $x'$  and  $\varphi'$  and that the curve moves vertically when  $\ln q$  changes.

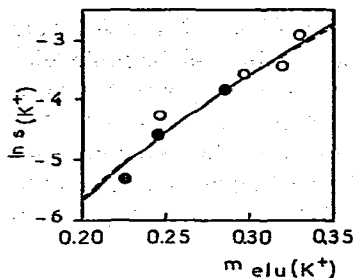


Fig. A8. Points: experimental plots of  $\ln s_{(K^+)}$  versus  $m_{e lu(K^+)}$  for cytochrome *c* reproduced from Fig. 4 in ref. 4. The continuous and broken curves are theoretical, obtained by giving best values of 9 and 13 to  $\varphi'$ , respectively.

(compare Fig. A7a and b with Fig. 9), the values of 13 and 9 for  $\varphi'$  obtained from the experiment with lysozyme would almost correspond to best values of 15 and 10 for  $\varphi$  obtained from the experiment with poly-L-lysine. Further, it was assumed that the value of  $\epsilon$  for lysozyme is equal to that obtained for poly-L-lysine (see column 7 in Table AII; *cf.*, Tables II and III); for  $\sigma$ , several values between 1 and 10 were assumed. As lysozyme is a rigid molecule and as the value of  $\epsilon$  can be considered to be large enough for the molecule to be adsorbed virtually in the energetically most stable configuration (or configurations) (see Discussion), the value of  $\sigma$  would represent the number of energetically most stable configurations of the molecule on the crystal surface [see Theoretical (Section A)]. It can be seen in Table AII that the theoretical values of both  $x$  and  $\xi$  are not much influenced by the value of  $\sigma$ , however.

The points in Fig. A8 are experimental plots (corresponding to those in Fig. A7) for cytochrome *c* reproduced from Fig. 4 in ref. 4; two curves are theoretical, calculated by giving the best two values 13 and 9 (see above) to the parameter  $\varphi'$  and values that give the best fits with the experimental results to parameters  $x'$  and  $\ln q$ , which are given in columns 1 and 3 in Table AIII, respectively. In columns 6, 8 and 9 in Table AIII are given values of  $x\epsilon/kT$ ,  $x$  and  $\xi$  for cytochrome *c* estimated for the two most reasonable values of  $\varphi'$  and for several hypothetical values of  $\sigma$ . In this instance also, theoretical values of both  $x$  and  $\xi$  are not much influenced by the value of  $\sigma$ .

TABLE AIII  
PARAMETERS ESTIMATED FOR CYTOCHROME *c*

$x'$	$\varphi'$	$\ln q$	$\beta$ (assumed)	$\sigma$ (assumed)	$x\epsilon/kT$	$\epsilon$ (assumed) (kcal/mole)	$x$	$\xi$
$5.5 \pm 0.2$	13	9.5	$4.79 \cdot 10^{-2}$	1	12.5	2.03	3.6	0.65
				2	11.9		3.5	0.64
				4	11.2		3.3	0.60
				10	10.2		3.0	0.55
$6.4 \pm 0.2$	9	9.1	$2.46 \cdot 10^{-2}$	1	12.8	2.20	3.4	0.53
				2	12.1		3.3	0.52
				4	11.4		3.1	0.48
				10	10.5		2.8	0.44

Finally, it should be recalled that theoretical curves in Figs. A7 and A8 were calculated by taking into account the fact that the  $R_F$  or the  $B$  value<sup>4</sup> of the molecules before the molarity gradient of potassium ions begins (*i.e.*, when the potassium concentration is 0.0015  $M$ ) is virtually zero, which was verified experimentally. This can be verified also from Tables AII and AIII: by using values in Tables AII and AIII and eqn. 1 in ref. 4, it can be shown that the  $B$  values of the molecules at a potassium concentration of 0.0015  $M$  are close to zero, *i.e.*,  $0.8 \cdot 10^{-3}$ – $1.4 \cdot 10^{-3}$  for lysozyme and  $0.8 \cdot 10^{-4}$ – $1.2 \cdot 10^{-4}$  for cytochrome *c*.

#### ACKNOWLEDGEMENTS

The author is grateful to Dr. G. Bernardi for useful discussions and interest in this work, and thanks the Délégation Générale à la Recherche Scientifique et Technique, Paris, for financial support. Calculations were performed on a CDC 6600 computer of the Faculty of Sciences, University of Paris.

#### REFERENCES

- 1 G. Bernardi, *Nature (London)*, 206 (1965) 779.
- 2 G. Bernardi, *Methods Enzymol.*, 21 (1971) 95.
- 3 G. Bernardi and T. Kawasaki, *Biochim. Biophys. Acta*, 160 (1968) 301.
- 4 T. Kawasaki, *J. Chromatogr.*, 93 (1974) 313.
- 5 T. Kawasaki, *J. Chromatogr.*, 93 (1974) 337.
- 6 T. Kawasaki, *J. Chromatogr.*, 120 (1976) 271.
- 7 T. Kawasaki, *J. Chromatogr.*, 151 (1978) 95.
- 8 G. Bernardi, M. Giro and C. Gaillard, *Biochim. Biophys. Acta*, 278 (1972) 409.
- 9 G. Bernardi, *Methods Enzymol.*, 27 (1973) 471.
- 10 T. Kawasaki, *J. Chromatogr.*, 82 (1973) 219.
- 11 M. A. Kay, R. A. Young and A. S. Posner, *Nature (London)*, 204 (1964) 1050.
- 12 K. Sudarsanan and R. A. Young, *Acta Crystallogr.*, B25 (1969) 1534.
- 13 R. A. Young, *Colloques Internationaux CNRS No. 230: Physico-chimie et Cristallographie des Apatites d'Intérêt Biologique (Paris)*, C.N.R.S., Paris, 1973, p. 21.
- 14 D. R. Taves and R. C. Reedy, *Calcif. Tissue Res.*, 3 (1969) 284.
- 15 G. Bernardi, *Biochim. Biophys. Acta*, 91 (1964) 686.
- 16 G. Bernardi, *Methods Enzymol.*, 22 (1971) 325.
- 17 P. Doty and W. B. Gratzler, in M. A. Stahmann (Editor), *Polyamino Acids, Polypeptides and Proteins*, University of Wisconsin Press, Madison, Wisc., 1962, p. 111.
- 18 T. Kawasaki, *J. Chromatogr.*, 82 (1973) 167.
- 19 T. Kawasaki and G. Bernardi, *Biopolymers*, 9 (1970) 257.
- 20 T. Kawasaki, *J. Chromatogr.*, 82 (1973) 237.
- 21 T. Kawasaki, *J. Chromatogr.*, 82 (1973) 191.
- 22 B. E. Conway, *Electrochemical Data*, Elsevier, Amsterdam, 1952, pp. 76–77 and 86.
- 23 E. Daniel and Z. Alexandrowicz, *Biopolymers*, 1 (1963) 473.
- 24 R. C. Weast, *Handbook of Chemistry and Physics*, Chemical Rubber Co., Cleveland, Ohio, 52nd ed., 1971–1972, p. F171.
- 25 C. Y. C. Pak and F. C. Bartter, *Biochim. Biophys. Acta*, 141 (1967) 410.
- 26 J. Applequist and P. Doty, in M. A. Stahmann (Editor), *Polyamino Acids, Polypeptides and Proteins*, University of Wisconsin Press, Madison, Wisc., 1962, p. 161.
- 27 Y. W. Tseng and J. T. Yang, *Biopolymers*, 16 (1977) 921.
- 28 H. Kuhn, W. H. Kuhn and A. Silberberg, *J. Polym. Sci.*, 14 (1954) 193.
- 29 R. B. Corey and L. Pauling, *Proc. Roy. Soc. London, Ser. B*, 141 (1953) 10.
- 30 K. Lonsdale, *Nature (London)*, 217 (1968) 56.
- 31 G. Montel, *Colloques Internationaux CNRS No. 230: Physico-chimie et Cristallographie des Apatites d'Intérêt Biologique (Paris)*, C.N.R.S., Paris, 1973, p. 13.
- 32 W. E. Brown, *Nature (London)*, 196 (1962) 1048.